Marine Pollution Bulletin 210 (2025) 117303

Contents lists available at ScienceDirect

Marine Pollution Bulletin

journal homepage: www.elsevier.com/locate/marpolbul

Sources and distribution of organic matter and polycyclic aromatic hydrocarbons in sediments of the southwestern Portuguese shelf

Mário Mil-Homens [a,b,*], Sofia Gonçalves [b], Alejandro Cortés [c], Barend L. van Drooge [c], Henko de Stigter [d], Joan O. Grimalt [c], Lívia Gebara Cordeiro [e,f], Miguel M. Santos [b,g], C. Marisa R. Almeida [b,h], Miguel Caetano [a,b]

[a] IPMA, Divisão de Oceanografia e Ambiente Marinho, Instituto Português Do Mar da Atmosfera, I.P., Avenida Doutor Alfredo Magalhães Ramalho, 6, 1495-165 Algés, Portugal
[b] CIIMAR/CIMAR-LA, Centro Interdisciplinar de Investigação Marinha e Ambiental, Universidade do Porto, Terminal de Cruzeiros de Leixões, Av. General Norton de Matos s/n, 4450-208 Matosinhos, Portugal
[c] Institute of Environmental Assessment and Water Research (IDAEA-CSIC), c/Jordi Girona, 18-26, 08034 Barcelona, Catalonia, Spain
[d] NIOZ, Royal Netherlands Institute for Sea Research, Department of Ocean Systems, Landsdiep 4, 1797SZ 't Horntje, Texel, the Netherlands
[e] IPMA, Divisão de Geologia e Georecursos Marinhos, Instituto Português Do Mar da Atmosfera, I.P., Avenida Doutor Alfredo Magalhães Ramalho, 6, 1495-165 Algés, Portugal
[f] CCMAR, Centro de Ciências do Mar, Universidade do Algarve, Campus de Gambelas, 8005-139 Faro, Portugal
[g] Departamento de Biologia, Faculdade de Ciências da Universidade do Porto, Rua do Campo Alegre s/n, 4169-007 Porto, Portugal
[h] Departamento de Química e Bioquímica, Faculdade de Ciências da Universidade do Porto, Rua do Campo Alegre, 687, 4169-007 Porto, Portugal

ARTICLE INFO

Keywords:
Marine sediments
Organic matter composition
Stable carbon and nitrogen isotopes
Perylene
USEPA-16ΣPAHs

ABSTRACT

Total organic carbon (C_{org}), total nitrogen (N_{tot}), C_{org}/N_{tot}, $\delta^{13}C_{org}$, $\delta^{15}N$, calcium carbonate ($CaCO_3$), and grain size were analyzed in 70 surface samples and 19 short cores from the southwestern Portuguese shelf. Perylene and USEPA-16 PAHs were quantified in a subset of these samples. The findings suggest that organic matter derives from a mix of terrestrial and marine sources, outlined by C_{org}, N_{tot}, and isotopic signatures. Perylene combined with $\delta^{13}C_{org}$ was used to identify the main PAH sources in these environments. Diagnostic perylene ratios revealed contributions from natural sources in the Tagus region and contaminated materials from the Sado Dredged Disposal Site, with additional perylene in Sines linked to atmospheric deposition of pyrogenic sources. A significant correlation between perylene and USEPA-16 PAHs indicates natural and anthropogenic inputs from the Tagus. This multiproxy approach—combining USEPA-16ΣPAHs, perylene, and $\delta^{13}C_{org}$—offers insights for assessing environmental risks and guiding marine environmental management according to the MSFD.

1. Introduction

Organic matter (OM) in coastal sediments may originate from both terrestrial and marine sources, including autotrophic and heterotrophic organisms, as well as anthropogenic compounds (e.g., Schmidt et al., 2010). The OM accumulated in these environments is highly dependent on the source inputs, physical sorting by marine hydrodynamic processes, and biogeochemical transformations that may involve remineralisation both in the water column and sediments (Xia et al., 2022). The physical dynamic processes involve the resuspension of sedimentary organic matter and the degradation in the overlying water column, which influences on the accumulation and burial of organic matter in coastal waters (Sun et al., 2024).

In industrialized and urbanized coastal areas, polluted OM may originate from sewage effluents, domestic, farming and industrial activities (Liu et al., 2015; Rumolo et al., 2011). The released contaminants may attach to certain components of the sediment, such as fine-grained mineral and organic matter particles, due to their surface properties and the increase in surface area with decreasing particle size (Birch, 2020; Logemann et al., 2023). The accumulation of contaminants can lead to significant and abrupt changes in the marine environment, threatening the sustainability of ecosystems. (Abessa et al., 2005; Moreno-González et al., 2015; Viñas et al., 2010).

The incorporation processes of contaminants trapped both in sinking

* Corresponding author at: IPMA, Divisão de Oceanografia e Ambiente Marinho, Instituto Português Do Mar da Atmosfera, I.P., Avenida Doutor Alfredo Magalhães Ramalho, 6, 1495-165 Algés, Portugal.
E-mail address: mario.milhomens@ipma.pt (M. Mil-Homens).

https://doi.org/10.1016/j.marpolbul.2024.117303
Received 10 September 2024; Received in revised form 1 November 2024; Accepted 12 November 2024
Available online 25 November 2024

organic matter and sedimentary organic matter also depend on its composition, e.g. marine or terrestrial (Bianchi et al., 2002). Marine OM is mostly composed of labile components that are easily degraded by heterotrophic microorganisms, whereas terrestrial OM is derived from soils and plants, which are generally more refractory (Burdige, 2007).

Different OM sources can be identified based on their bulk elemental (carbon and nitrogen) and isotopic ($\delta^{13}C_{org}$ and $\delta^{15}N_{tot}$) compositions (Zhao et al., 2019). The combination of bulk OM parameters such as C_{org}/N, $\delta^{13}C_{org}$ and $\delta^{15}N_{tot}$ is useful to trace the origin, fate and temporal variability of sedimentary OM in estuarine and marine environments (Andrews et al., 1998; Gao et al., 2012; Heyes et al., 2006; Rumolo et al., 2011). These parameters are important for identifying sources assuming that the bulk elemental and isotopic ratios of sedimentary OM are consistent and respond linearly to physical mixing among the end-members (Andrews et al., 1998; Gao et al., 2012; Heyes et al., 2006).

Further understanding on the source and transport pathways of OM can be obtained by analysing specific molecular organic compounds. Polycyclic aromatic hydrocarbons (PAHs) are a group of organic molecules primarily of anthropogenic origin and due to their toxic, carcinogenic and mutagenic properties are considered of environmental concern (Zhang et al., 2020; Zhang et al., 2014). PAHs are widely present in the environment, and are used as geochemical markers to assess anthropogenic influences in specific environments (Pang et al., 2022) as well as in natural processes (e.g., wildfires, natural oil seep in sediments,

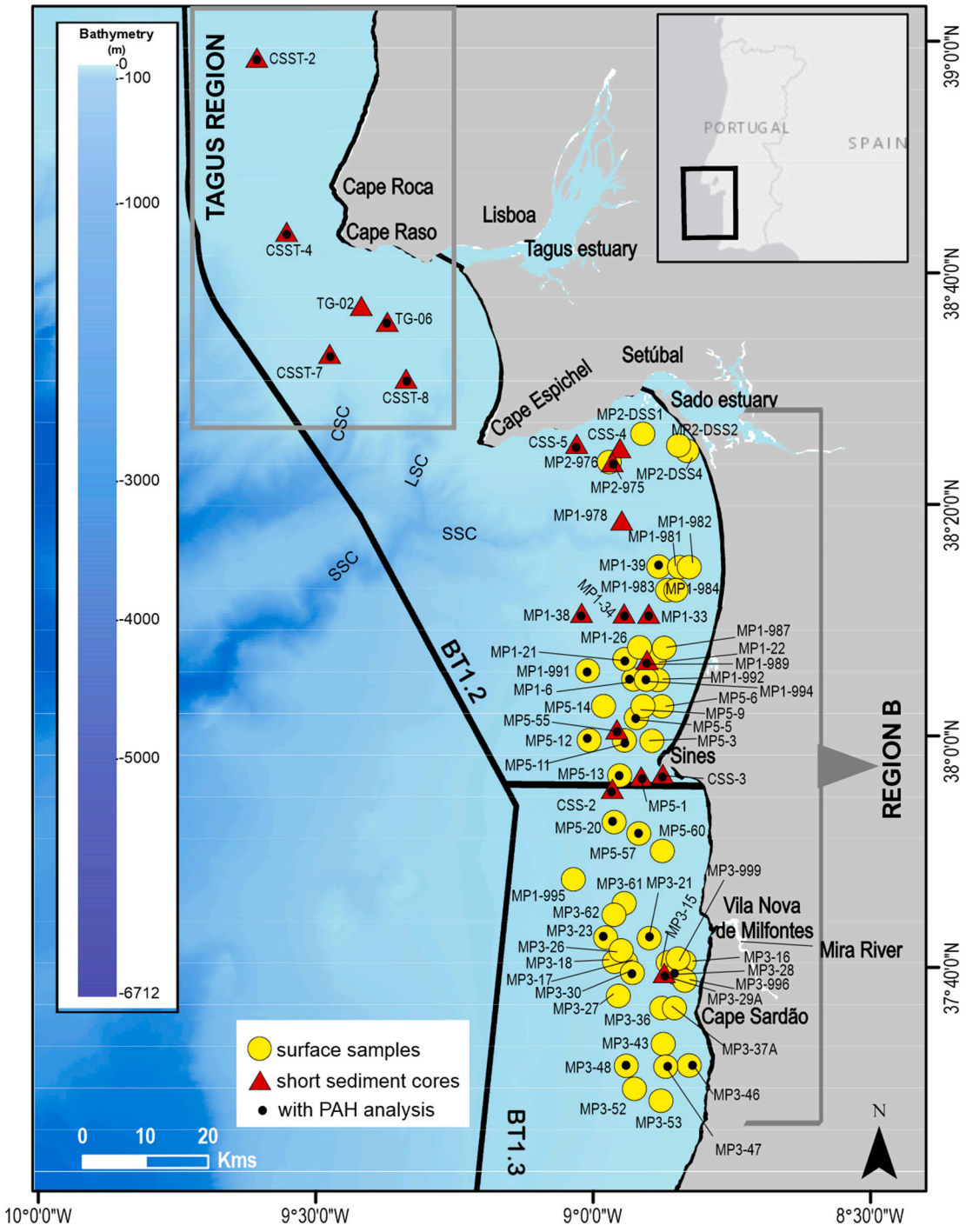

Fig. 1. Map of the sediment sampling locations. Thick black lines represent the limits of the MSFD regions.

diagenetic or thermal maturation processes) (Zakrzewski et al., 2020). They are produced by the incomplete combustion of organic matter through natural phenomena (e.g., forest fires) or human activities (e.g., direct release of oil and oil products, combustion of biomass and fossil fuels) (Chen et al., 2006; Simpson et al., 1996). PAHs can be grouped into three types: pyrolytic PAHs (combustion-derived), petrogenic PAHs (petroleum-derived) and diagenetic PAHs (derived from biogenic precursors in sediment). Perylene, a five-ring polycyclic aromatic hydrocarbon, is widely distributed in the environment. It is often found alongside other man-made PAHs, but it can come from different sources or environmental processes, indicating diverse depositional conditions (Lima et al., 2003; Silliman et al., 2000). Specifically, perylene is associated with terrestrial OM derived from fungal activity in forest soils (Gocht et al., 2007; Hanke et al., 2019), suggesting that it can serve as a terrestrial proxy for river inputs (Hu et al., 2014). Other authors propose that perylene can be produced by early diagenesis of algal and crinoids precursors (Liu et al., 2012; Venkatesan, 1988; Wakeham et al., 1979). It can also be generated by human-made combustion processes (Venkatesan et al., 1998). Due to their hydrophobic nature, low vapour pressure and high octanol-water partition coefficient, PAHs have a greater tendency to adsorb to suspended particles (Chen et al., 2024).

In Portugal, scarce information is available on the composition of organic matter and PAHs in marine sediments. The present study describes a set of sedimentary organic matter parameters (C_{org}, N_{tot}, C_{org}/N_{tot} ratio, $CaCO_3$, $\delta^{15}N$, $\delta^{13}C_{org}$) and the 16 priority USEPA polycyclic aromatic hydrocarbons (USEPA-16ΣPAHs), including perylene for the first time, in region BT1.2 and most BT1.3 of the South Western Portuguese shelf (Fig. 1). The former area, the present study is aimed to provide information 1) on the origin and composition of OM over the recent past accumulated on the southwestern Portuguese continental shelf, in the area that did not reach the Good Environmental Status (GES) in the first Marine Strategy Framework Directive (MSFD) evaluation report and the second fulfilled it satisfactorily (MAMAOT, 2012). The information collected in the present study describes the origin and composition of the OM deposited in the recent past, including its role in PAH distribution and its potential role in the transport of organic contaminants (e.g., PAHs) from land to coastal areas. This baseline study may provide useful information for environmental policies and regulations aimed to reduce the burden of contaminants in the marine environments.

2. Materials and methods

2.1. Sampling area

The study area corresponds to the BT1.2 area and part of the BT1.3. The former is located near the Tagus and Sado estuaries and the port of Sines. The northern one (Fig. 1), is characterized by a relatively wide shelf (ca. 20–34 km) which comprises the shelf of Estremadura Spur in the north and the Tagus shelf extending between Cape Roca and Cape Espichel in the south. The Tagus River, the longest river of the Iberian Peninsula, debouches on this northern segment via the Tagus estuary. The shelf area adjacent to the Tagus estuary is characterized by prodelta encompassing large muddy sediment patches between 50 and 130 m water depth. Its fine-grained deposit is composed of sediments of both fluviatile and marine origin (Gaspar and Monteiro, 1977; Jouanneau et al., 1998; Lima, 1971).

The southern segment, here referred to as Region B, extends from Cape Espichel to Cape Sardão and is marked by a fairly narrow (10–20 km) shelf and a steeper gradient than the northern counterpart (Vanney and Mougenot, 1981). The relatively small Sado River debouches in this area forming a small fine-grained sediment deposit is found in the shelf area adjacent to the Sado estuary (Jouanneau et al., 1998). The Setúbal submarine canyon (SSC) incises the shelf seawards from the mouth of the Sado estuary. The LSC connects to SSC as a tributary at around 2000 m water depth (mwd), and the SSC continues downslope until it reaches the Tagus Abyssal Plain at around 4840 mwd, 175 km from the canyon head (Arzola et al., 2008).

The Tagus River represents the main source of freshwater input in the area, with distinct dry/wet seasonal and inter-annual variability. The mean discharge flow of the Tagus River close to the river mouth is about 500 $m^3\ s^{-1}$ estuary (Benito et al., 2003), while the Sado and Mira Rivers contribute 40 and 10 $m^3\ s^{-1}$, respectively (Vale et al., 1993; Ferreira et al., 2003). All three rivers end in tidal estuaries. The Tagus estuary is the largest in Europe with an area of 330 km^2. The Sado and Mira estuaries encompass about 160 km^2 and 3 km^2, respectively (Caetano et al., 2016). All three estuaries are characterized by intense farming. Additionally, past mining activities of the Iberian Pyrite Belt formations were also developed in these areas.

Lisboa and Setúbal, 545,000 and 123,000 inhabitants, respectively, are the two largest population centres in the adjacent land area. Sines has the largest port in Portugal and is one of the main hubs for container transhipment on the Atlantic and Mediterranean routes. Additionally, the area contains an oil refinery and a thermoelectric power plant, which was decommissioned at the end of 2021 (Cobelo-García et al., 2011; Costa et al., 2011; Jouanneau et al., 1998; Mil-Homens et al., 2013; Mil-Homens et al., 2009). The Sado estuary has a shipyard, a paper mill and a petrochemical complex that continue to operate. A chlor-alkali plant, a pyrite roast plant, a smelter and a shipyard in the Tagus estuary ended its activity in the eighties (Caeiro et al., 2005; Canário et al., 2005; Figueres et al., 1985; Rocha and Palma, 2019).

All the western Portuguese shelf is characterized by seasonal coastal upwelling during spring and summer, induced by the steady northern winds (Fiúza, 1983). In its northern part the irregular coastal and submarine morphology (e.g., Estremadura Spur, Cape Roca and Cape Espichel, Cascais (CSC), Lisboa (LSC) and Setúbal (SSC) submarine canyons), result in a complex upwelling system with active centres and shadow areas (Moita et al., 2003). Coastal convergence (downwelling) dominates during the cold seasons (Fiúza et al., 1982) taking place when the wind stress that acts on the sea surface is oriented northwards. Summer is marked by a low-energy wave regime (ca. 2 m significant wave height), while the winter shows a high-energetic condition with significant wave heights exceeding 5 m (Quaresma et al., 2007).

2.2. Sediment sampling

The sediment samples investigated were collected in the southwestern Portuguese continental shelf in two oceanographic campaigns, March 2019 and 2021, onboard of the Noruega and the NRP Almirante Gago Coutinho research vessels, respectively (Fig. 1, Table SM1 and Table SM2). A Smith McIntyre grab, a multicorer and a boxcorer were used. On-board, the surface sediments (0–2 cm) from the Smith McIntyre grab were subsampled, while the sediment cores from the multicorer and box-corer were sub-sectioned in different depth intervals, with 1 cm resolution in the top 4 cm, 2 cm resolution between 4 and 20 cm core depth, and 3 cm resolution below 20 cm core depth. Samples were stored cool at 4 °C. In the laboratory, subsamples for the various types of analysis (C_{org} and N_{tot} and their stable isotopes $\delta^{13}C_{org}$ and $\delta^{13}N_{tot}$, ^{210}Pb, ^{226}Ra, grain-size) were freeze-dried. The subsamples for chemical and isotopic composition analysis were sieved through a 2 mm mesh to remove shells and other coarser material, and then milled using agate pots in a Fritsch Pulverisette 7 Classic Line planetary mill.

2.3. Sample analysis

2.3.1. Sediment core dating

The ^{210}Pb and ^{226}Ra determinations were measured as described elsewhere (Haffert et al., 2020). Briefly, the α-spectrometry determinations were performed on 500 mg of freeze-dried ground and homogenized sediment which was spiked with 1 mL of standard solution of ^{209}Po in 2 M HCl and leached with 10 mL of concentrated HCl for 6 h at 85 °C in a water bath. For electrochemical deposition, 45 mL of

demineralized water were added to the solution with 5 mL of ascorbic acid ($C_6H_8O_6$) solution (4 % *w/v*). The Po-isotopes (natural ^{210}Po and added ^{209}Po) were deposited on suspending silver plates added to the solution. Canberra Passivated Implanted Planar Silicon detectors were used for α-spectrometry.

For the γ-spectrometry, a small amount of freeze-dried and homogenized sediment sample was placed in a 5 cm diameter plastic petri dish, which was then sealed with tape and placed in a gas-tight plastic envelope. After allowing the sample to reach equilibrium for at least 4 weeks, we used a Canberra Broad Energy Range High Purity Germanium (BEGe) detector to measure ^{210}Pb and ^{226}Ra. The 46.5 keV line was used for the former and 295.2, 351.9, and 609.3 keV lines for the latter. The detector was connected to a computer by a digital spectrum analyzer (DSA-1000) and the radionuclide activities were counted using Genie 2000 gamma spectroscopy software. The detector was calibrated externally using a Geological Certified Reference Material IAEA/RGU-1, dated 1 January 1988. A monitor standard IAEA-300 was used for quality control.

Sediment chronology was based on the down-core distribution of ^{210}Pb (half-life 22.3 years) determined indirectly by α-spectrometry measurement of its granddaughter ^{210}Po in 12 samples per core. ^{226}Ra, as proxy of supported ^{210}Pb ($^{210}Pb_{supported}$), was determined in 3 samples per core by γ-spectrometry. The difference between total ^{210}Pb activity obtained by α-spectrometry and the average ^{226}Ra activity ($^{210}Pb_{supported}$) in each sediment core was taken to represent the excess ^{210}Pb. The estimation of sedimentation rates was based on fitting a Constant Flux and Constant Sedimentation Rate model (Carpenter et al., 1982) including a surface mixed layer (SML) CF/CS + SML on the observed ^{210}Pb down-core profiles, as generally performed for ^{210}Pb profiles marked by a relatively slow downward decline in excess ^{210}Pb activity in the biologically mixed surface sediment layer followed by a more noticeable exponential downward decline in the deeper subsurface sediment layer (Boer et al., 2006). The sedimentation rate was estimated from the ^{210}Pb decline in the layer below the surface mixed layer.

2.3.2. Grain size

About 5 g of each lyophilized and homogenized sediment sample were pre-treated with 150 mL of H_2O_2 (30 % solution) and 1.5 mL of NH_3 to oxidize the OM, in a water bath at 60 °C, until the end of the reaction. Samples were then oven-heated at 65 °C for 24 h, washed three times with ultrapure water and centrifuged to remove excess reagent. After addition of 1.5 mL of sodium hexametaphosphate (CALGON) to avoid flocculation of clays, the coarse fraction (>2 mm) was removed by wet sieving. The grain-size distribution (from 0.04 to 2000 μm) was determined by laser diffraction using a Coulter LS-1320. The measurements were replicated three times for data consistency. The median values were reported as volume % of the fraction <63 μm.

2.3.3. Elemental and stable isotope analysis

Total carbon (C_{tot}) and nitrogen (N_{tot}) contents were determined by high-temperature combustion on a Leco Truspec micro-analyzer CHNS. For the determination of inorganic carbon (C_{inorg}), samples were first heated in a muffle furnace for 3 h at 400 °C to combust OM. The C_{org} was calculated from the difference between C_{tot} and C_{inorg} content. Three replicate subsamples of 2 mg of each dried and homogenized sediment sample were measured, before and after combustion. The relative precision of repeated measurements was lower or equal to 0.03 % (dry weight). Assuming that inorganic carbon occurs predominantly in the form of calcite and aragonite, the $CaCO_3$ content (in percent) was obtained by multiplying the weight percentage of inorganic carbon by 8.3 (de Stigter et al., 2007). The C_{org}/N_{tot} ratio was calculated considering the ratio between organic carbon and total nitrogen on weight basis.

Stable isotopes of carbon ($\delta^{13}C_{org}$) and nitrogen ($\delta^{15}N_{tot}$) were measured directly using an Organic Elemental Analyzer, Flash 2000, coupled to an Isotopic Ratio Mass Spectrometer (IRMS), Delta V Advantage via Conflo IV. Each sample was analyzed in duplicate (relative standard deviation of the measured duplicates was all within ±10 %). The $\delta^{15}N_{tot}$ values were determined directly on bulk powdered samples. For the analysis of stable carbon isotopes ($\delta^{13}C_{org}$), 200 mg of sample were pre-treated with 2.5 mL HCl (1 M) and agitated at room temperature for 24 h to remove the carbonates. Samples were then washed with ultrapure water, centrifuged three times to neutralize the sample, and freeze-dried to remove the water. Data quality control was checked by running the certified reference materials (CRMs) in each day of analysis. The CRMs used were USGS-24 and USGS-40 for $\delta^{13}C_{org}$ and IAEA-N1, IAEA-N2 and IAEA-NO3 for $\delta^{15}N$. The relative error in percentage of the 9 measurements of each CRM was 2.8, 0.5, 4.3, a.4 and 0.4, respectively. The raw measurements of samples and all standards used were normalized relative to CRMs, namely USGS-24 (−16.05 ‰) and USGS-40 ($\delta^{13}C$ -26.39 ‰; $\delta^{15}N$ -4.52 ‰) for carbon and IAEA-N1 (+0.4 ‰), IAEA-N2 (+20.3 ‰) and IAEA-NO3 (+4.7 ‰) for nitrogen. All the isotope data were reported in the conventional delta notation relative to the Vienna Pee Dee Belemnite (VPDB). The results are given in parts per mil (‰).

2.3.4. Analysis of polycyclic aromatic hydrocarbon (PAH)

The concentrations of polycyclic aromatic hydrocarbons (PAHs) were determined following the method described in Van Drooge et al. (2011). In brief, 5 g of freeze-dried sediment from each sample were added to centrifuge tubes and spiked with 25 μL of a 16PAH-deuterated standard mix (1 ng/μL for each surrogate compound). They were extracted with 25 mL CH_2Cl_2/MeOH (2:1) in an ultrasonic bath (3 × 15 min). After each extraction and centrifugation, the supernatant was transferred into a glass balloon. Then, the complete extract was reduced to 5 mL by rotary-evaporation, and 6 mL of KOH/MeOH (6 %) was added to the balloon to hydrolyse the extract overnight. PAHs were extracted with n-hexane (3 × 10 mL) from the hydrolysed extract using a liquid-liquid method, and the combined supernatant was transferred to a 100 mL flask. The extract was then concentrated to 1 mL using a rotary evaporator and loaded onto a 1 g Al_2O_3 column. Elution was carried out using a 2 mL mixture of CH_2Cl_2 and hexane (2:1), and the eluate was collected in a 50 mL glass flask. After rotary-evaporation to 1 mL, the sample was transferred to a vial and further concentrated to 100 μL under a gentle N_2 stream. Subsequently, 1 μL of the concentrated sample was injected into a GC–MS (Agilent 5975) equipped with a fused silica capillary column (HP-5MS Agilent Technologies; 60 m length, 0.25 μm film thickness, and 0.25 mm internal diameter). Helium was used as carrier gas at a flow rate of 1.1 mL/min. The oven temperature was initially set to 90 °C for 1 min, then increased at a rate of 10 °C/min until reaching 120 °C, and finally increased at a rate of 6 °C/min until reaching 320 °C, where it was held for 15 min. The transfer line, injection port and ion source temperatures were set at 300 °C, 280 °C and 200 °C, respectively. The analyses were conducted in SIM mode for the PAHs listed in Table SM3. The PAH concentrations were adjusted for blank levels, which were within the range of the Limit of Detection of the methodology, ranging from 0.01 to 0.09 ng/g (dry weight) (Table SM3). Identification was performed by using the EPA Mix 9 standard and the retention index method. Quantification was performed using calibration curves for each compound (detector response vs amount injected standard and surrogate compound), except benzo(*e*)pyrene and perylene, that were measured by reference to deuterated benzo(*a*)pyrene. All measurements were performed in the ranges of linearity found of each compound. The quantitative data were corrected for surrogate recoveries of the deuterated compounds which were between 65 % and 82 %.

2.4. Statistical data analysis

The statistical treatment was performed independently in the Tagus region and Region B (Fig. 1). Box-and-whisker plots were calculated for each variable in the two groups of samples. The Spearman correlation coefficient was used to determine the relationships between the studied

parameters (C_{org}, fine fraction, N_{tot}, $\delta^{15}N_{tot}$ and $\delta^{13}C_{org}$, perylene and USEPA-16ΣPAHs). The normality of the C_{org} and N_{tot} data in the two regions was assessed using the Shapiro-Wilk tests ($p > 0.05$; Statistica version 14.0). Differences between the two sampling groups were tested using the Mann-Whitney *U* Test (non-parametric).

3. Results

3.1. Sediment core chronology

The profiles of total ^{210}Pb activity ($^{210}Pb_{tot}$) versus sediment depth are represented in Fig. 2. The highest $^{210}Pb_{tot}$ activities were observed in the top 5 cm sediment from the Tagus region, ranging from 125 mBq/g to 355 mBq/g. In this region, the lowest total ^{210}Pb activity was measured in core TG-06. This core, collected near the Tagus river mouth at relatively shallow water depth of 71 m, had the coarsest median grain-size when compared to the others from this region (see grain-size data). Core CSST-7 (collected around 130 mwd) exhibited the highest total ^{210}Pb activity.

The collected sediment cores displayed relatively low and constant ^{226}Ra activities (used as proxy for supported ^{210}Pb activity) with depth (Table 1). These values were in good agreement with previous studies obtained in the region (de Stigter et al., 2007; Mil-Homens et al., 2009; Mil-Homens et al., 2006). The down-core profiles of $^{210}Pb_{tot}$ showed surface mixed layers (SML) reaching depths of 2 to 10 cm (Table 1). These SML can be attributed to natural sediment mixing by bioturbation and anthropogenic mixing resulting from bottom trawling, anchoring, dredging, and dumping operations. These processes can modify the physical (e.g., grain size), chemical (e.g., OM degradation) and biological properties of the sediments. The occurrence of species, such as the crustacean *Callianassa subterranea* in the Portuguese shelf sediments can explain the relatively large thickness of the SMLs reaching 9–10 cm in several sediment cores (Table 1). This species lives in sandy-muddy bottom sediments (Sampaio et al., 2016) and is capable of excavating burrows that can reach several tens of cm deep (Ziebis et al., 1996). In cores TG-06 (sampling location nearest to the Tagus river mouth) and CSS-3 (collected inside the Sines harbour) $^{210}Pb_{tot}$ activity showed only little decrease with depth (Fig. 2), suggesting fast sedimentation.

3.2. Grain-size, $CaCO_3$, C_{org} and N_{tot} contents

The surface samples and down-core samples of the Tagus shelf region showed significantly higher contents of fine fraction in the Region B samples (Fig. 3a, Fig. 4a and Fig. SM1). The median fine fraction content this region was around 80 % (Fig. 3a), increasing down-core to 89 %, with the lowest content found in core TG-06 (Fig. 4a). In Region B, the fine-fraction contents in the surface samples were only similar to those found in the Tagus shelf only in core CSS-3 (inside of the Sines harbour) and in core CSS-5 collected near the Sado dredged material disposal site (DMDS) (Fig. 3a).

No gravel-sized material was observed in the sediment cores from the Tagus region. The surface samples in Region B (ca. 65 samples) and in short cores were dominated by sand with relatively low quantities of gravel (mean contents around 2 %), except in five cases that had gravel contents around 25 % (MP3-999, MP2-976, MP1-982, MP1-984, MP5-3). The gravel was mainly composed of biogenic calcium carbonate debris.

The calcium carbonate ($CaCO_3$) contents were generally low in the Tagus region (Fig. 3d and Fig. SM1d). In this region, the highest contents were found in the surface samples of cores CSST-2 and CSST-4, located further away from the Tagus mouth. The highest $CaCO_3$ contents were also found in the vicinities of Vila Nova de Milfontes (Mira mouth). The surface samples containing the highest $CaCO_3$ contents were

Table 1
Length of the studied sediment cores, thickness of the surface mixed layer (SML), sedimentation rate (SR in cm/yr), and ^{226}Ra activity. n.p.e. means not possible to estimate.

Region	Cores ID	Length (cm)	SML (cm)	SR (cm/yr)	^{226}Ra (mBq/g)
Tagus region	CSST-2	32	10	0.16	28 ± 4
	CSST-4	26	9	0.42	33 ± 4
	TG-06	28	n.p.e	n.p.e	41 ± 1
	TG-02	35	6	0.72	34 ± 1
	CSST-7	26	2	0.98	31 ± 2
	CSST-8	23	6	0.26	37 ± 1
"Region B"	CSS-5	19	5	0.15	23 ± 3
	CSS-4	12	9	0.11	16 ± 3
	MP2-975	16	6	0.14	19 ± 2
	MP1-978	18	7	0.12	34 ± 11
	MP1-33	16	7	0.09	14 ± 2
	MP1-34	25	9	0.03	22 ± 4
	MP1-38	17	9	0.05	14 ± 3
	MP1-989	21	7	0.15	19 ± 2
	MP5-55	18	6	0.12	30 ± 2
	MP5-1	13	9	0.17	13 ± 5
	CSS-2	14	11	0.03	20 ± 2
	CSS-3	21	n.p.e.	n.p.e.	20 ± 2
	MP3-29A	31	8	0.15	13 ± 3

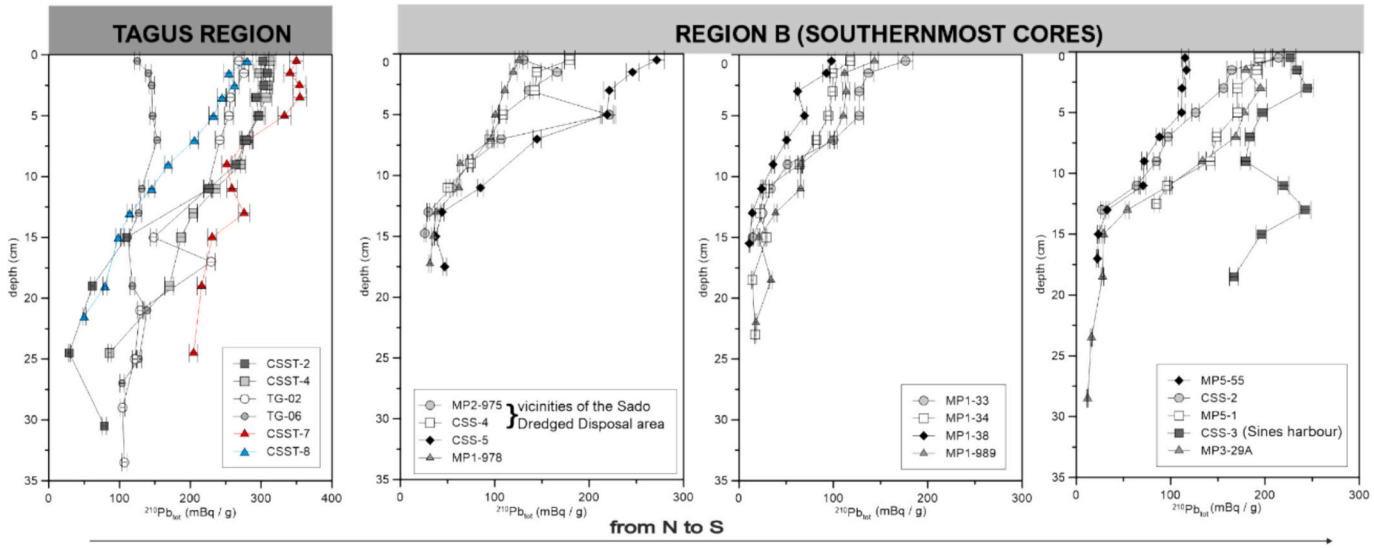

Fig. 2. Distribution of total ^{210}Pb activity with depth in the studied sediment cores.

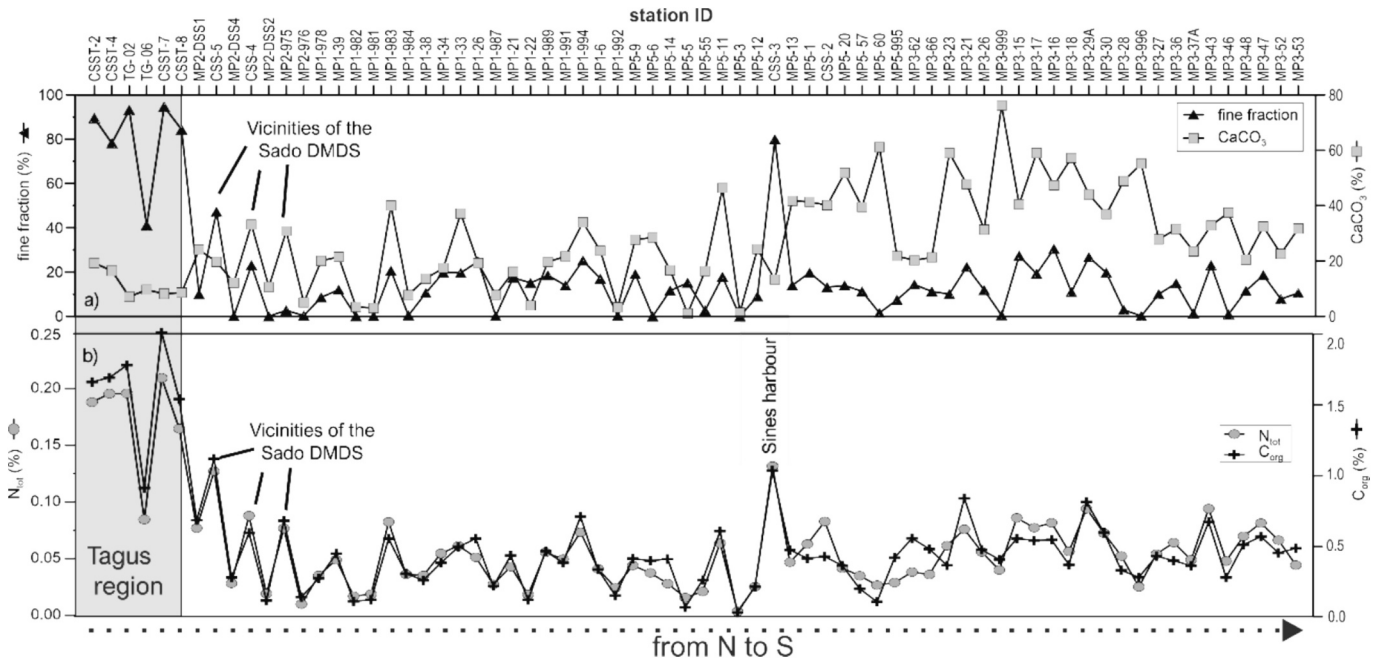

Fig. 3. Spatial variation of fine fraction (%) and $CaCO_3$ (%) (a), and C_{org} (%) and N_{tot} (%) (b) in the collected surface sediments. The samples are ordered from North (left) to South (right). The shaded area indicates the samples collected from the Tagus region.

characterized by relatively low fine-fraction contents, suggesting that $CaCO_3$ was mainly present in coarser-grained biogenic (shells and foraminifera) debris.

The spatial distributions of C_{org} and N_{tot} paralleled the distribution of the fine fraction (Fig. 3, Fig. SM1a-b, Fig. 4a-c), with the highest values observed in the Tagus shelf and the lowest in the remaining locations further north and south. The same general pattern of low $CaCO_3$ and high C_{org} and N_{tot} contents in surface sediment of the Tagus region was found in the sediment column (Fig. 4a-d), with rather uniform downcore distributions (Fig. SM3 and Fig. SM4).

The Shapiro-Wilk test showed statistically significant differences between both regions in the surface and downcore samples (Table SM4). The Mann-Whitney *U*-Test for non-normally distributed variables showed that the fine fraction, $CaCO_3$, C_{org}, and N_{tot} distributions in the two regions were significantly different, involving fine fraction U = 25, 11, 33 and 169, respectively ($p < 0.05$ in all cases). The observed $CaCO_3$, C_{org} and N_{tot} contents in the Tagus region were in good agreement with those obtained in previous studies in this part of the Portuguese margin (Alt-Epping et al., 2007; Costa et al., 2011; Mil-Homens et al., 2009).

3.3. $\delta^{15}N_{tot}$ and $\delta^{13}C_{org}$ of sedimentary organic matter

The median $\delta^{15}N_{tot}$ values of 5.1 ‰ (range from 4.7 ‰ to 5.8 ‰) in the sediments from the Tagus region were slightly higher than those from Region B, 4.7 ‰ (range from 2.4 ‰ to 7.1 ‰), respectively (Fig. 5). The $\delta^{13}C_{org}$ in the samples from the Tagus and B regions ranged from −26.4 ‰ to −20.3 ‰ (median value of −23.5 ‰) and from −24.2 ‰ to −20.3 ‰ (median value of −21.8 ‰), respectively (Fig. 5). These values were in good agreement with those obtained previously in surface samples collected in the Tagus prodelta region (Alt-Epping et al., 2007).

The surface and down-core samples sediments from the Tagus region had a different $\delta^{15}N_{tot}$ and $\delta^{13}C_{org}$ signatures from those of Region B (Mann-Whitney *U* Tests U = 1930 and U = 448, respectively, $p < 0.05$). Both $\delta^{15}N_{tot}$ and $\delta^{13}C_{org}$ distributions were significantly non-normal (Table SM4). In the two regions the values of $\delta^{13}C_{org}$ and $\delta^{15}N_{tot}$ were not correlated with C_{org} content (Tagus region Spearman correlation coefficient $r = -0.19$, $p = 0.05$; Region B $r = 0.01$, $p = 0.05$) suggesting that the sedimentary organic material had a high level of heterogeneity due to multiple sources.

The uniform down-core trends of these two parameters suggests a rather constant input through time (Fig. SM3 and Fig. SM4). Core TG-06, from near the Tagus river mouth, constituted an exception, with approximately constant values of $\delta^{15}N_{tot}$ and $\delta^{13}C_{org}$ from the bottom of the core up to 15 cm depth, followed by an increase towards the surface (Fig. SM5). Unfortunately, the ^{210}Pb results did not allow establishing the sedimentation chronology at this core location (see sub-section 3.1).

3.4. Concentrations of perylene and the USEPA-16ΣPAHs

The highest concentrations of perylene and USEPA-16ΣPAHs were observed in sediments of the Tagus shelf area (Fig. 6 and Fig. 7). In the Tagus region perylene ranged from 4 to 408 ng/g (median 64 ng/g), while in Region B varied from 1 to 55 ng/g (median 4.5 ng/g) (Fig. 6b). The highest concentrations of perylene and USEPA-16ΣPAHs were found in core TG-06 collected in the shelf area adjacent to the Tagus river mouth (Fig. 6, Fig. 7 and Fig. SM2).

As is the case of the other parameters studied, the concentrations of perylene and the USEPA-16ΣPAHs showed, in general, small down-core variability (Fig. 7a Fig. 7b). However, it is possible a slight increase of these compounds was observed in cores CSST-2, CSST-4, CSST-8 and MP2–975 (Fig. SM3 and Fig. SM4) as well as a decrease in core TG-06 (Fig. SM5). These two variables and the fine fraction and C_{org} contents had a similar spatial and down-core variabilities. In the upper 10 cm of core TG-06 a decrease in the concentrations of perylene and PAHs was observed, following the trend of decreasing fine fraction and C_{org} content. However, the high values at sub-surface (2–3 cm depth), where both the fine-fraction and C_{org} content showed little changes (Fig. SM5), suggests that other factors than grain-size or organic carbon were responsible for these enrichments.

Very few previous studies on PAH concentrations (Rocha and Palma, 2019; Rocha et al., 2017) in marine sediments from the Portuguese shelf area available. The concentrations of perylene and PAHs in the surface sediment collected near the Tagus river mouth (TG-06, CSST-7 and CSST-8) were much higher than the values found by Rocha and Palma (2019), e.g., perylene and PAHs concentrations of 54 and 171 ng/g, respectively, in the vicinities of TG-06 had.

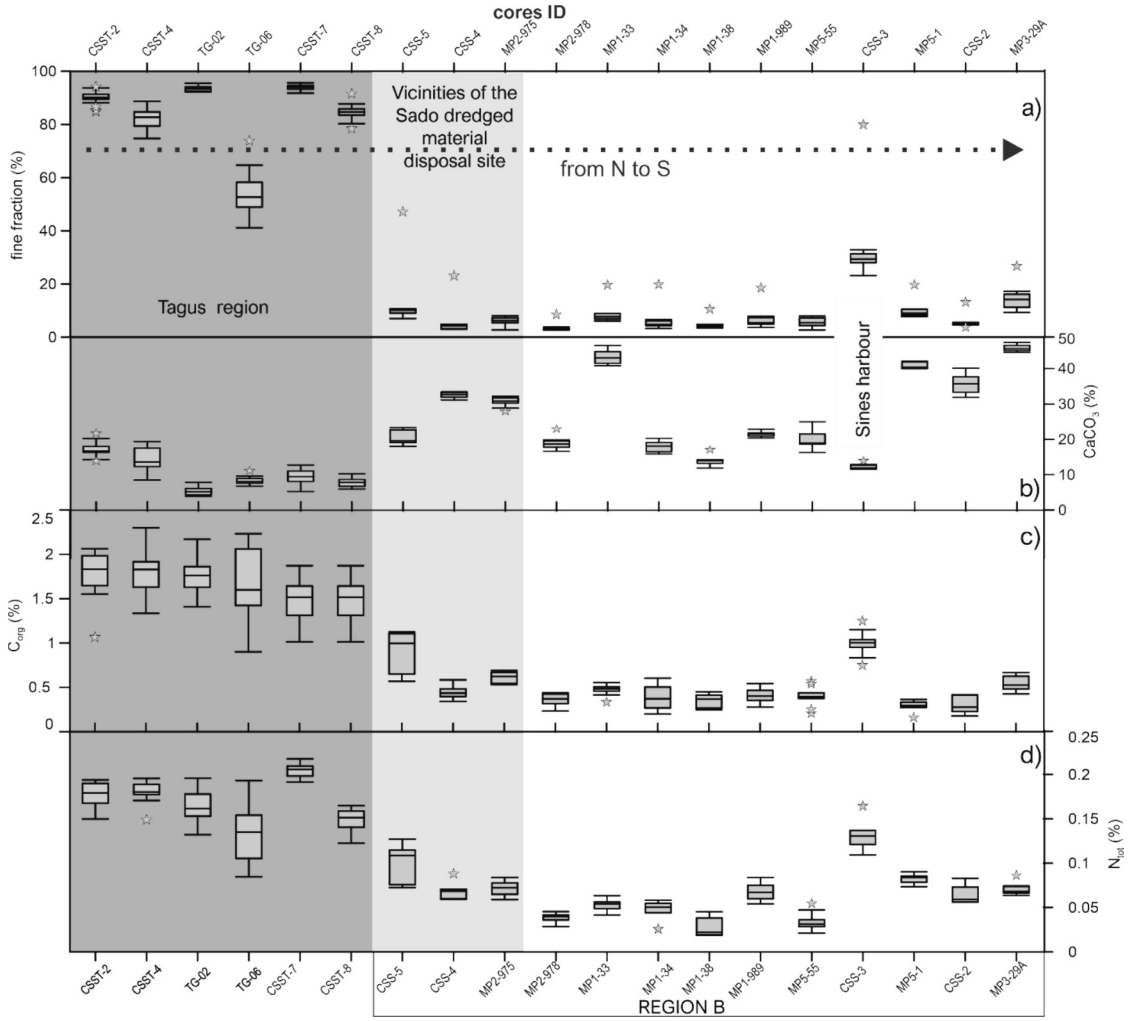

Fig. 4. Box-whisker plots of fine fraction (volume %) a), $CaCO_3$ (% *w*/w) b), C_{org} (%) c) and N_{tot} (%) d) in the studied sediment cores, ordered from North (left) to South (right). Dark and light grey shading indicate the samples collected in the Tagus region and in the vicinities of the Sado dredged material disposal site, respectively. The box-whisker plots show minimum, maximum, median, and lower and upper quartiles. The box represents the interquartile range that contains 50 % of the values. The line across the box indicates the median, and the whiskers the 95 % of high and low confidence interval. The stars represent outlier that are defined as 1.5 times the interquartile range.

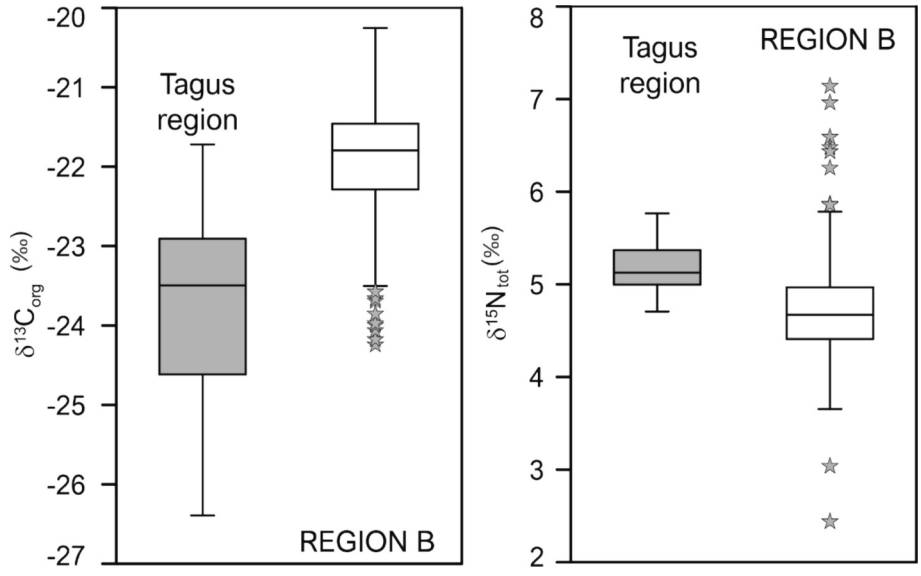

Fig. 5. Box-whisker plots for the $\delta^{13}C_{org}$ a) and $\delta^{15}N_{tot}$ b) in the studied sediment samples. The star symbol refers to outliers.

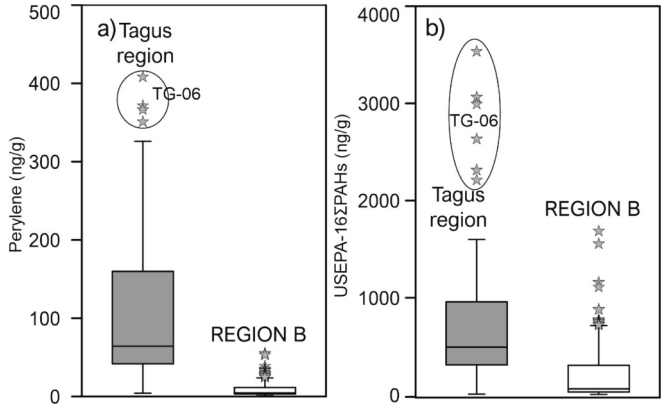

Fig. 6. – Box-whisker plots for the perylene a) and USEPA-16ΣPAHs b) in the studied sediments. The star symbols represent outlier samples.

In both regions, the USEPA-16ΣPAHs distributions were significantly not normally distributed in both regions (Table SM4; Figures SM3-SM5). The Mann-Whitney *U* Test showed that USEPA-16ΣPAHs and perylene distributions were significantly different (U = 884 and 216, respectively, $p < 0.05$). In both areas the concentrations of USEPA-16ΣPAHs and perylene were significantly correlated (Tagus region Spearman correlation coefficient $r = 0.97$, $p < 0.05$; Region B $r = 0.86$, $p < 0.05$), suggesting the same transport pathway or similar input sources. However, no positive correlation of perylene and PAH with the sediment fine fraction and C_{org} was observed in the Tagus region suggesting that the variability of PAHs in sediment of the Tagus region was mostly related to variations in sources and emissions than being dependent on the sediment composition (fine fraction and C_{org}).

4. Discussion

4.1. Grain-size, $CaCO_3$, C_{org} and N_{tot} distributions

The high concentration of fine-grained sediment in the Tagus area could be attributed to significant export of estuarine particulate matter from the Tagus estuary. As distance from the estuary increased, the influence of its sediment transfers diminished, particularly in areas with higher $CaCO_3$ content, as observed in the more distant cores CSST-2 and CSST-4. This indicated that the fine-grained terrestrial contributions in the Tagus region diluted the $CaCO_3$ content, which is likely of marine biogenic origin. The low fine-fraction content in core TG-06 could be due to the higher hydrodynamic energy associated with its shallower depth, leading to the winnowing of fine-grained particles.

The high fine-fraction content observed inside the Sines harbour likely reflected the relatively low hydrodynamic energy that allowed the deposition of these fine-grained particles. In other cores from Region B, the fine-fraction content was consistently higher at the surface compared to further down-core, suggesting the presence of transient fine sediment deposits that are winnowed out and exported to adjacent areas over longer time spans. The finer-grained core tops were considered statistical outliers (Fig. 4a). While the mouth of the Tagus estuary is relatively sheltered from ocean waves incident from the north-westerly direction, the winnowing might also be the result of internal waves generated at the nearby edge of the Lisboa Submarine Canyon (LSC) that propagate onto the shelf, as described in the Nazaré Submarine Canyon (Quaresma et al., 2005).

In Region B, the relatively coarser sediments reflected from

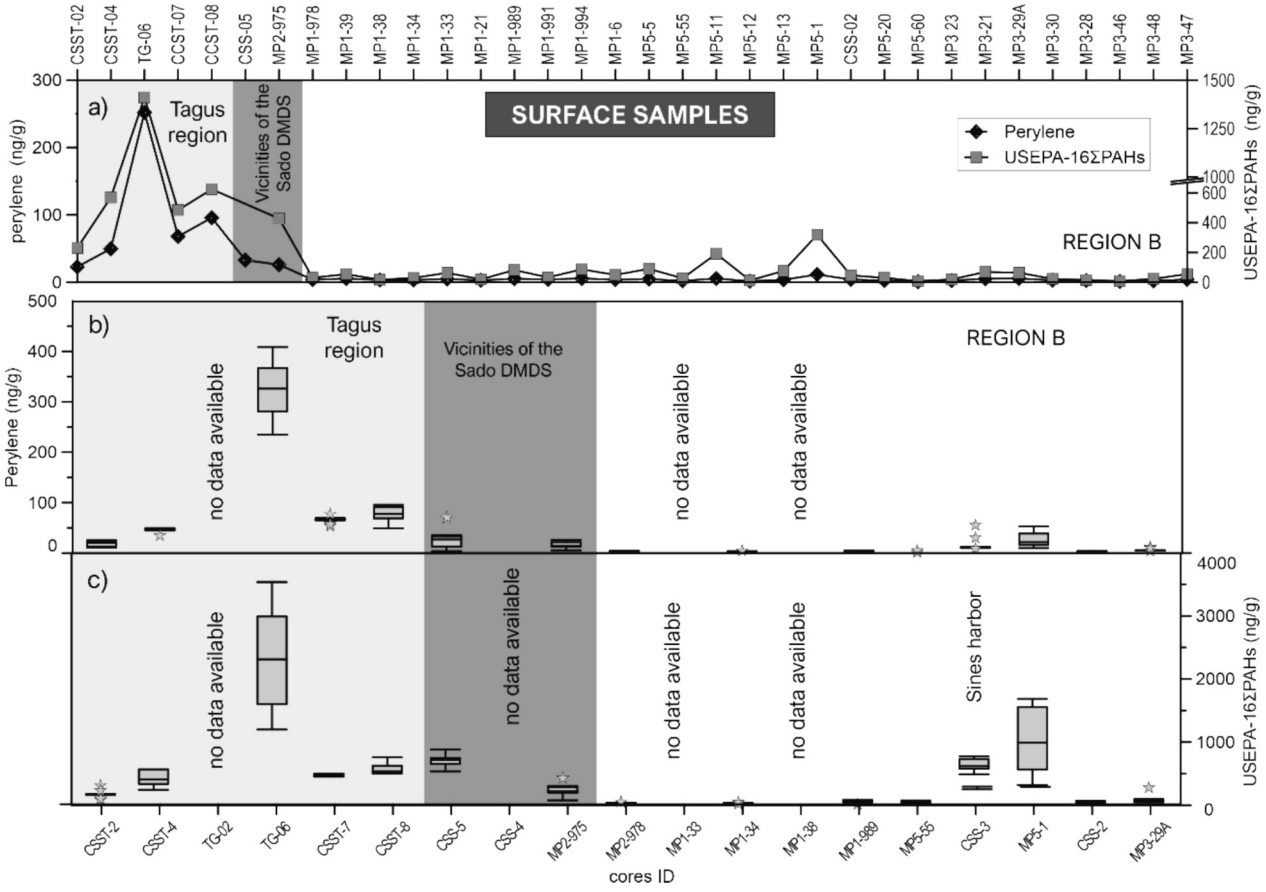

Fig. 7. Spatial variation of perylene and USEPA-16ΣPAHs in the surface samples (a). Box-whisker plots for the perylene b) and USEPA-16ΣPAHs c) in the collected sediment cores, ordered from North (left) to South (right). The star symbol represents outlier samples. No data available refer to lack of measurements in these cores.

hydrodynamic conditions that were vigorous enough to mobilize fine-grained particles and the low discharges from the Sado and Mira rivers, and consequently low export of fine-grained particles to the coastal area. The similarity of the spatial distribution pattern of C_{org}, N_{tot} and fine fraction confirmed the trend of OM to accumulate with fine material (Mayer, 1994), in contrast to $CaCO_3$ that tended to be found in sand.

4.2. Assessing the characteristics of organic matter in marine sediments using C_{org}/N_{tot} and $\delta^{13}C_{org}$

4.2.1. Variability pattern of C_{org}/N_{tot}

The C_{org}/N_{tot} ratio is commonly used as a tool for distinguishing terrestrial and marine organic matter in sediments (Stein, 1991). The range of organic carbon-total nitrogen ratio (C_{org}/N_{tot}) for marine OM varies between 4 and 10, this ratio is higher than 15 in terrestrial plants which is attributed to the presence of cellulose (Meyers, 1997; Meyers, 1994). The presence of cellulose in most land plants, adding up to their relative C content, explains the higher C_{org}/N_{tot} ratios in terrigenous OM. This ratio is >20 when vascular land plants prevail (Meyers, 1994). The presence of significant inorganic nitrogen (adsorbed on clay minerals) and/or the occurrence of fractionation processes during OM degradation may modify the C_{org}/N_{tot} ratio, limiting the use of this ratio as an indicator of OM source in marine sediments (Meyers, 1997; Schubert and Calvert, 2001).

Representation of N_{tot} vs C_{org} in the sediments of the Tagus region (Fig. 8) showed a high positive intercept of nitrogen (0.06 %) with zero organic carbon (C_{org}), which may indicate the occurrence of inorganic sedimentary nitrogen in sediments that can be bound as ammonium ions to clay particles, especially illite (Fig. 8) (Schubert and Calvert, 2001; Stein and Rack, 1995). The regression line (in green) for the N_{tot} and C_{org} from Region B crosses very close to the axis origin (refer to Fig. 5), suggesting that nitrogen in the sediment was mainly present in the form of organic compounds. Therefore, N_{tot} can be used as an estimation of organic nitrogen (N_{org}) (Goñi et al., 1998; Hedges et al., 1988). According to these regression plots 38 % and 69 % could be explained in terms of the content of C_{org} in the Tagus region and Region B.

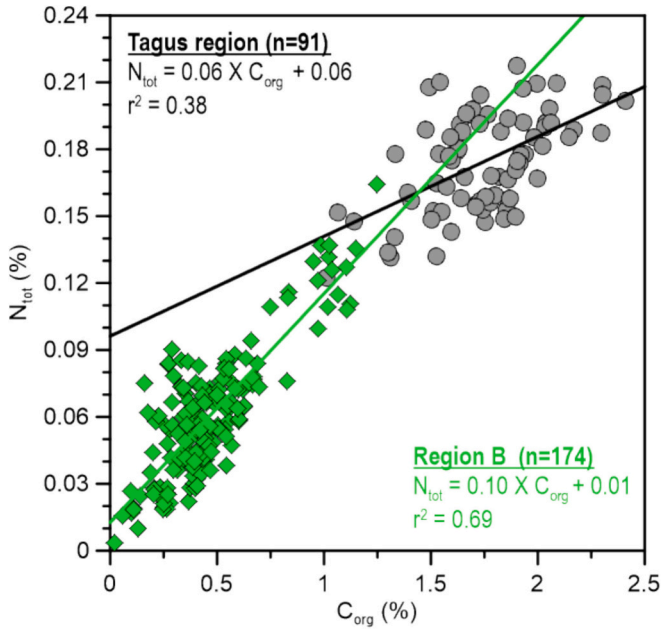

Fig. 8. Relationship between total nitrogen (N_{tot}) and organic carbon (C_{org}) in the two studied regions. The solid grey and green lines represent the linear regression of the samples from the Tagus region and B region, respectively. (For interpretation of the references to colour in this figure legend, the reader is referred to the web version of this article.)

Thus, a substantial part of N_{tot} was associated with other nitrogen forms. Lima (1971) found that illite is the dominant clay mineral in the clay fraction between Cape Raso and Cape Espichel (see locations in Fig. 1), particularly in the most offshore areas of this shelf sector (range between 34 and 66 % and median 49 %). The C_{org}/N_{tot} ratios of the surface samples from the Tagus region and Region B ranged from 12 to 37 (median 13) and from 4 to 14 (median 8), respectively (Fig. 9). Hence, the OM in the former could be derived predominantly from terrestrial inputs, whereas that of the Region B was mostly of marine origin. Consistently, core TG-06 (nearest to the Tagus river estuary mouth, Fig. 1) had the highest C_{org}/N_{tot} ratio. Consequently, the predominance of OM from marine sources in surface samples of Region B was consistent with the relatively minor discharges from lower Sado and Mira rivers. The samples with extremely low (<3.5) C_{org}/N_{tot} ratios (4 out 8) were mostly from core MP5–1 (located offshore Sines harbour, see Fig. 1), characterized by low contents of C_{org}, possibly due to the efficient degradation or low deposition of organic matter at this location. Also in the subsurface sediment samples, the C_{org}/N_{tot} values were highest in the Tagus region (Fig. 10). Still, no down-core variability was observed in the uniform C_{org}/N_{tot} ratios.

4.2.2. Spatial and temporal distribution of $\delta^{13}C_{org}$ and $\delta^{15}N_{tot}$

Marine OM is generally more enriched in $\delta^{13}C_{org}$ and $\delta^{15}N_{tot}$ than terrestrial OM (Lamb et al., 2006). The values of $\delta^{13}C_{org}$ in C3, C4 plants, and marine phytoplankton range, from −30 ‰ to −24 ‰ (average around −27 ‰), −16 ‰ to −10 ‰ (average around −13 ‰), and − 22 ‰ to −19 ‰ (average around −20.5 ‰), respectively (Meyers, 1994). On the other hand, the $\delta^{13}C$ values of sewage effluents may vary from −26 ‰ to −22 ‰ overlapping both terrestrial and marine sources (Barros et al., 2010). Early diagenesis has minimal impact on the carbon isotope composition of sinking and recently deposited OM. Accordingly, the isotopic signature of the sources is largely preserved in the sedimentary OM (Rumolo et al., 2011).

Marine organic matter (OM) is typically isotopically heavier than terrestrial OM due to phytoplankton uptake (Schubert and Calvert, 2001), with bulk $\delta^{15}N_{tot}$ values between 3 ‰-12 ‰ (Owens, 1988) and 5 ‰-7 ‰ in phytoplankton (Lamb et al., 2006). Nitrogen-fixing terrestrial plants produce OM around zero $\delta^{15}N_{tot}$, while those using soil minerals usually have positive values (Gao et al., 2012; Lamb et al., 2006). Therefore, terrestrial OM averages 2 ‰-3 ‰, with a range of −10 ‰ to 10 ‰. Wastewater treatment leads to heavier $\delta^{15}N_{tot}$ values, with livestock wastewater ranging from 10 ‰ to 25 ‰ (Wang et al., 2018). Untreated sewage effluents show $\delta^{15}N_{tot}$ values from 1.8 ‰ to 3.8 ‰ (Sampaio et al., 2010), while agricultural fertilizers can lower these values below 1.2 ‰ (Barros et al., 2010).

Bi-plots of $\delta^{15}N_{tot}$ vs $\delta^{13}C_{org}$ (Fig. 11a and b) and $\delta^{13}C_{org}$ vs C_{org}/N_{tot} (Fig. 12a and b) were used to get further information on the OM sources in the two regions. Typical $\delta^{15}N_{tot}$, $\delta^{13}C_{org}$ values and C_{org}/N_{tot} ratios for marine OM range, from 5 to 7 ‰, from −18 to −24 ‰ and from 4 to 10, respectively (Lamb et al., 2006). OM produced by C3 vascular plants has an average $\delta^{13}C_{org}$ value of −27 ‰ and C_{org}/N_{tot} ratios higher than 15 (Meyers, 1997).

The median $\delta^{13}C_{org}$ values (−21.8 ‰) and C_{org}/N_{tot} ratio (8.0) in sediments from Region B were found within the range of marine algae. The overall heavier (more negative) $\delta^{13}C_{org}$ values and higher C_{org}/N_{tot} ratios in sediments from the Tagus shelf, and especially in core TG-06, might reflect a greater contribution of C3 plants to OM in the sediments of this region, which was consistent with the highest river input in this shelf area. This contribution decreased with increasing distance from the Tagus river and was consistent with the highest C_{org}/N_{tot} ratio (37) in the TG-06 surface sample. Although the core TG-06 had a lower fine fraction and C_{org} content than other cores from the Tagus region, indicating a regime of high hydrodynamic energy, the upward increase in $\delta^{15}N_{tot}$ and $\delta^{13}C_{org}$ values suggested a slightly increase of marine influence (Fig. 11a). The OM showed a strong signal of terrestrial

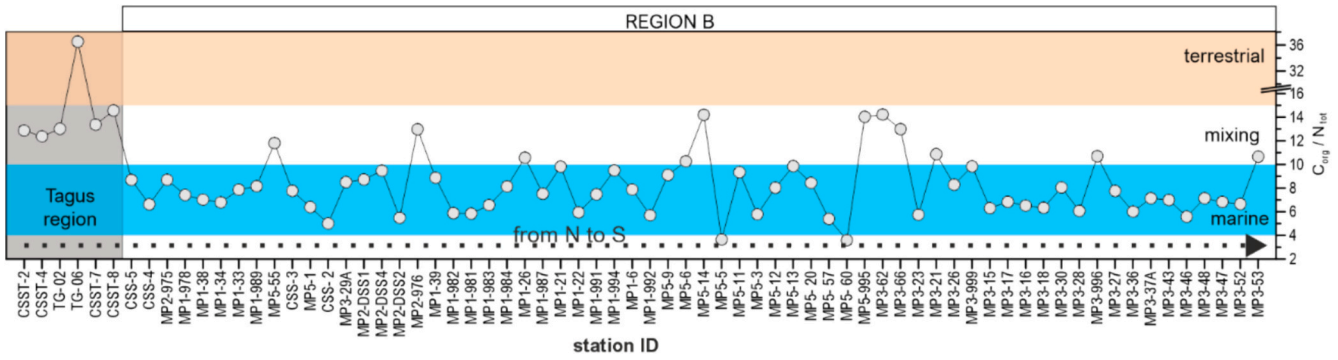

Fig. 9. Spatial variation of C_{org}/N_{tot} in the collected surface sediments. The samples are ordered from North (left) to South (right). The shaded area marks the surface sediment samples collected from the Tagus region. The light brownish and blue shaded bands represent the ranges of C_{org}/N_{tot} values of terrestrial and marine organic matter originated, as indicated in Meyers (1994, 1997). (For interpretation of the references to colour in this figure legend, the reader is referred to the web version of this article.)

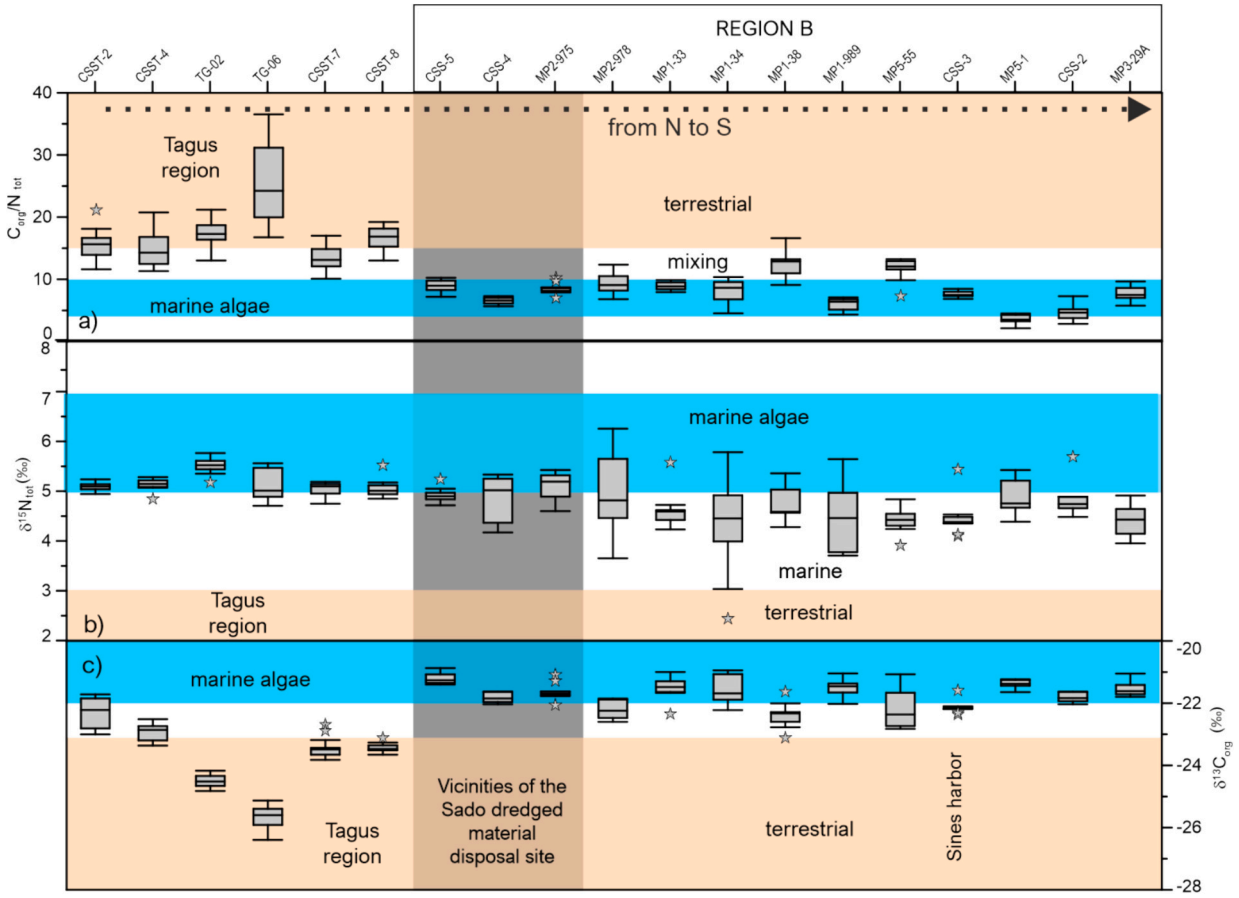

Fig. 10. Box-whisker plots for the C_{org}/N_{tot} ratios a), $\delta^{15}N_{tot}$ b) and $\delta^{13}C_{org}$ c), in the collected sediment cores, ordered from North (left) to South (right). The shaded area marks the cores collected from the Tagus region. The light brownish and blue shaded bands represent the ranges of C_{org}/N_{tot}, $\delta^{15}N_{tot}$ and $\delta^{13}C_{org}$ values of terrestrial and marine organic matter, after Meyers (1994, 1997). The star symbol represents outlier samples. (For interpretation of the references to colour in this figure legend, the reader is referred to the web version of this article.)

derived materials as suggested by the cross-plots of $\delta^{13}C_{org}$ vs C_{org}/N_{tot} (Fig. 12a) and $\delta^{13}C_{org}$ vs $\delta^{15}N_{tot}$ (Fig. 11a). The relatively lighter $\delta^{13}C_{org}$ in core CSST-2 (Fig. 10c), representing the northernmost sampling location of the Tagus region, suggests that the OM was a mixture of material from both marine and terrestrial sources, but with a lower contribution of OM derived from the Tagus river.

Surface samples (MP1-981, MP1-987, MP1-992, MP5-5, MP5-60, MP3-999 and MP3-996) with high $\delta^{15}N_{tot}$ values are characterized by relatively low contents of N and fine-fraction (Fig. SM2). These values are typical of marine OM (Owens, 1988).

4.2.3. *Quantification of OM sources*

The relative proportions of terrestrial allochthonous and marine autochthonous OM in the sediments of the southwestern Portuguese shelf can be estimated by application of the $\delta^{13}C$-based two end member mixing model (Perdue and Koprivnjak, 2007; Shultz and Calder, 1976). The proportion of terrestrial OM to total OM is expressed as T_{OM} (%) and calculated from the following eq. (1):

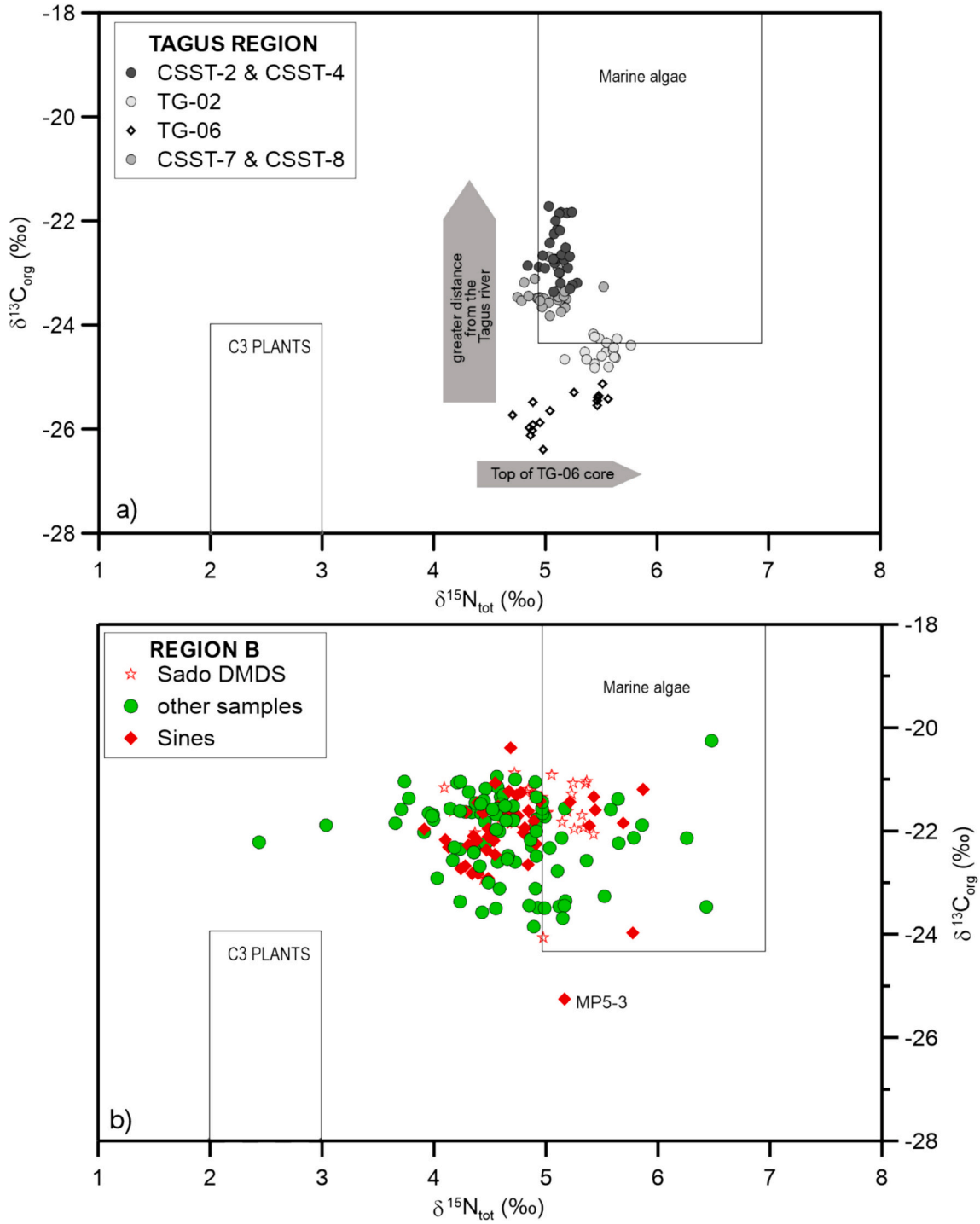

Fig. 11. $\delta^{13}C_{org}$ versus $\delta^{15}N_{tot}$ for sediment samples from a) the Tagus region and b) Region B.).

$$T_{OM}\ (\%) = \left(\left(\delta^{13}C_{org(mar)} - \delta^{13}C_{org(meas)}\right)/\left(\delta^{13}C_{org(mar)} - \delta^{13}C_{org(ter)}\right)\right) \text{ X } 100\% \quad (1)$$

where $\delta^{13}C_{org(meas)}$ is the measured carbon isotope composition, $\delta^{13}C_{org\ (ter)}$ and $\delta^{13}C_{org(mar)}$ are the terrestrial and marine end members, respectively. The contribution of marine OM (M_{OM}; %) to total OM was estimated by difference, according to the following eq. (2):

$$M_{OM}\ (\%) = 100 - T_{OM}\ (\%) \quad (2)$$

The value of the $\delta^{13}C_{org}$ terrestrial end member ($\delta^{13}C_{org(ter)}$) was chosen as −27 ‰, close to the lowest $\delta^{13}C_{org}$ value found in this study (−26.4 ‰) and in the middle of the stable carbon isotope range of terrestrial C3 plants (−30 to −24 ‰) (Gao et al., 2012; Liu et al., 2015; Winkelmann and Knies, 2005). Likewise, −20 ‰ was assumed as the $\delta^{13}C_{org}$ value of the marine end member. This value falls in the stable carbon isotopic range of marine phytoplankton (−22 to −19 ‰) given by Meyers (1997) and is in good agreement with the values reported by (Gao et al., 2012; Liu et al., 2015; Winkelmann and Knies, 2005).

Terrestrial organic matter (T_{OM}) dominated the two surface samples (TG-02 and TG-06) collected nearby the Tagus river mouth, reflecting the proximity of the terrestrial source. In the other surface sediment samples from the Tagus region, the relative contribution of terrestrial

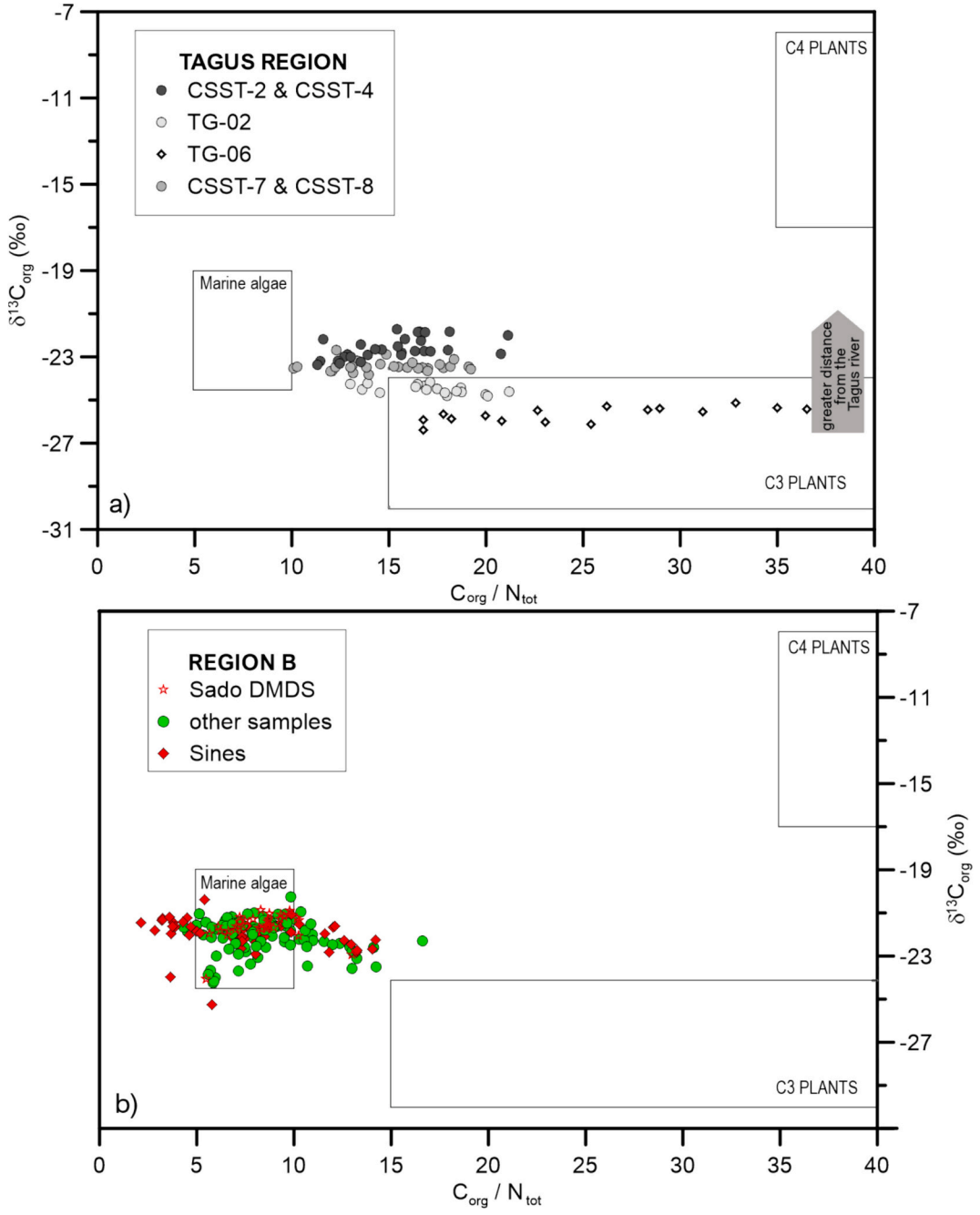

Fig. 12. $\delta^{13}C_{org}$ versus C_{org}/N_{tot} for sediment samples from a) the Tagus region and b) Region B.

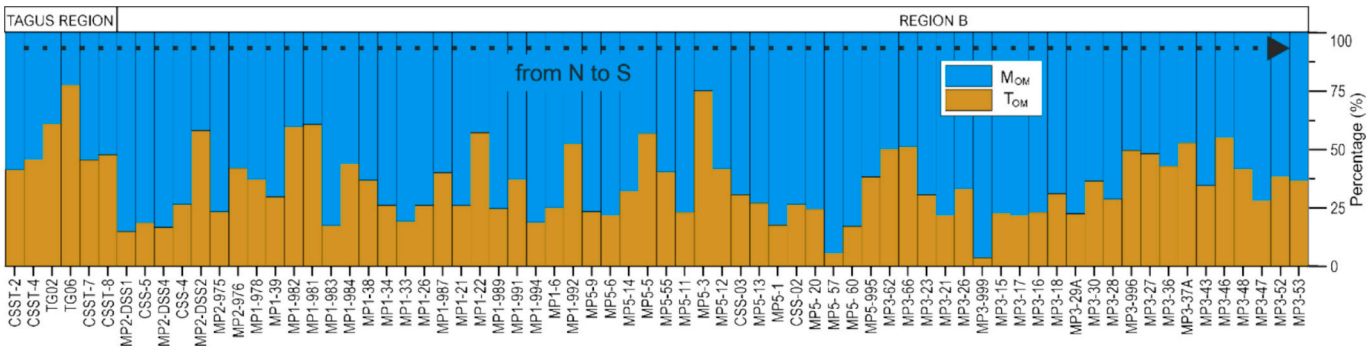

Fig. 13. Relative contribution of terrestrial OM (T_{OM}) and marine OM (M_{OM}) in the surface sediments.

OM was slightly lower than the marine-derived OM. In the surface samples of the region B, the marine-derived OM (OM_{mar}) was dominant, accounting for 67 ± 14 % (Fig. 13). The contribution of $C_{org(ter)}$ to C_{org} was predominant in the Tagus region (Fig. 13).

The down-core values of T_{OM} showed a similar pattern as in the surface samples. In the Tagus region, in particularly in cores TG-06, TG-02, CSST-7 and CSST-8, terrestrial OM was dominant (Fig. 14). The influence of terrestrial sources decreased with distance from the Tagus river, suggesting progressive dilution with marine OM. Although the contribution of terrigenous OM was lower in the Region B sediment cores, it is still substantial. It should be considered as C_{org} is one of the most relevant contaminant carriers.

4.3. Origin of perylene: anthropogenic vs. natural diagenetic

The spatial distribution pattern of perylene and USEPA-16ΣPAHs paralleled the distribution of the fine-fraction and C_{org} contents. In general, high concentrations corresponded to high fine-fraction and C_{org} contents. However, the highest value of both perylene and the USEPA-16ΣPAHs occurred in the subsurface sample of core TG-06. This core had a lower fine fraction and C_{org} content than others from the Tagus region (Fig. 3a). The relatively heavier $\delta^{13}C_{org}$ value found at this location (Fig. 10c) reflected the prevalence of terrestrial OM in the proximity of the river, enriched in contaminants (USEPA-16ΣPAHs derived from anthropogenic sources) as well as terrestrial materials (perylene, $\delta^{13}C_{org}$). In Region B, core MP5–1 collected in the vicinities of the Sine harbour also showed relatively high concentrations in both perylene and the USEPA-16ΣPAHs in very low contents of the fine fraction and C_{org}. In opposition to TG-06, the relatively lighter $\delta^{13}C_{org}$ value together with the C_{org}/N_{tot} found at this location (Fig. SM2) pointed to a marine OM. In this case, Sines with both perylene the USEPA-16ΣPAHs could be associated with atmospheric deposition of anthropogenic pyrogenic sources derived from the Sines chemical complex.

The concentration of perylene decreased with increasing distance from the Tagus river mouth (Fig. 15a and Fig. SM2c). This pattern was also observed in other coastal settings (Hu et al., 2014; Luo et al., 2006; Varnosfaderany et al., 2014), suggesting progressive dilution and/or oxidation of perylene downstream of the source (Li et al., 2022). The progressive decrease of both perylene and USEPA-16ΣPAHs from the Tagus shelf to open marine waters was consistent with a predominant terrestrial input mediated by the river discharges. In the Tagus region, this was also consistent with the negative correlation of perylene and USEPA-16ΣPAHs with $\delta^{13}C_{org}$ (Spearman correlation coefficient $r = -0.89$ and $r = -0.79$, $p < 0.05$) (Fig. 15c) and the positive correlation with the C_{org}/N_{tot} ratio. Neither the Tagus region nor Region B showed downcore perylene distributions increasing with depth, as reported in other areas (Chen et al., 2006; Silliman et al., 2000), which allowed to discard local early-diagenetic enrichment.

In Region B, no clear correlation was observed between $\delta^{13}C_{org}$ and perylene $\delta^{13}C_{org}$ (Fig. 15b) and USEPA-16ΣPAHs (Fig. 15d). Thus, in this region the perylene may not have a predominantly terrestrial origin but rather represent a mixture originating from natural biogenic diagenesis of marine precursors and anthropogenic inputs. Perylene and USEPA-16ΣPAHs wre significantly positively correlated with fine-fraction and organic carbon content (perylene: fine fraction $r = 0.57$, $p < 0.05$ & C_{org} $r = 0.57$, $p < 0.05$; USEPA-16ΣPAHs: fine fraction $r = 0.57$, $p < 0.05$ & C_{org} $r = 0.47$, $p < 0.05$), indicating the affinity of these compounds with organic matter and fine-grained sediment content and the role of the latter in the transport and dispersion of PAHs.

The origin of perylene, either natural or anthropogenic can also be assessed from the proportion of perylene relative to the sum of five-ring PAHs concentrations (Σ5-rings; benzo(*b*)fluoranthene, benzo(*k*)fluoranthene, benzo(*e*)pyrene, benzo(*a*)pyrene and perylene) and by the proportion of perylene relative to 17ΣPAHs. Values of perylene/Σ5-ring PAHs >10 % indicated a natural diagenetic origin, whereas <10 % suggests a probable anthropogenic pyrogenic origin (Bajt, 2022; Hu et al., 2014; Readman et al., 2002; Silliman et al., 2000). In the sediment samples from the Tagus region and Region B, the ratio between perylene/Σ5-ring PAHs ranged from 16 % to 36 % (median value 27 %) and from 8 % to 54 % (median value 21 %), respectively (Fig. 16a), suggesting that perylene was derived from natural early diagenetic sources (marine and terrestrial inputs) in the Tagus region and in most locations of Region B. Therefore, this compound can be used as a tracer for evaluating the contribution of the Tagus river inflow to PAH contamination originating from the estuary.

The lowest perylene/Σ5-ring PAHs, indicating possible anthropogenic pyrolytic origin, in this region were observed in the vicinities of Sines (cores MP5–1 and CSS-3, with median values of 9.7 % and 11 %, respectively) and in one of the sediment cores collected nearby the Sado DMDS (core CSS-5, median value of 11.1 %) (Fig. 16a). The Sado DMDS is a local deposition site of moderately contaminated sediment, derived from dredging in navigation channels, harbours, and shipyard facilities that is rated as Class 3 in the 5-class system that integrates the Portuguese regulation for dredged material quality assessment for trace metals (As, Cd, Cr, Cu, Hg, Ni, Pb and Zn) and persistent organic pollutants (e.g., PCBs, PAHs, HCB) (MAOTDR, 2007). Sediments with relatively high concentrations of the 5-ring PAH benzo(*b*)fluoranthene (72 ng/g) have been identified in the vicinities of the shipyards and a petrochemical complex located in the northern Sado river industrialized margin (Gonçalves et al., 2016).

For what concerns the proportion of perylene to 17ΣPAHs, a value of 1–4 % indicates that the source is pyrogenic (Bakhtiari et al., 2009; Fang

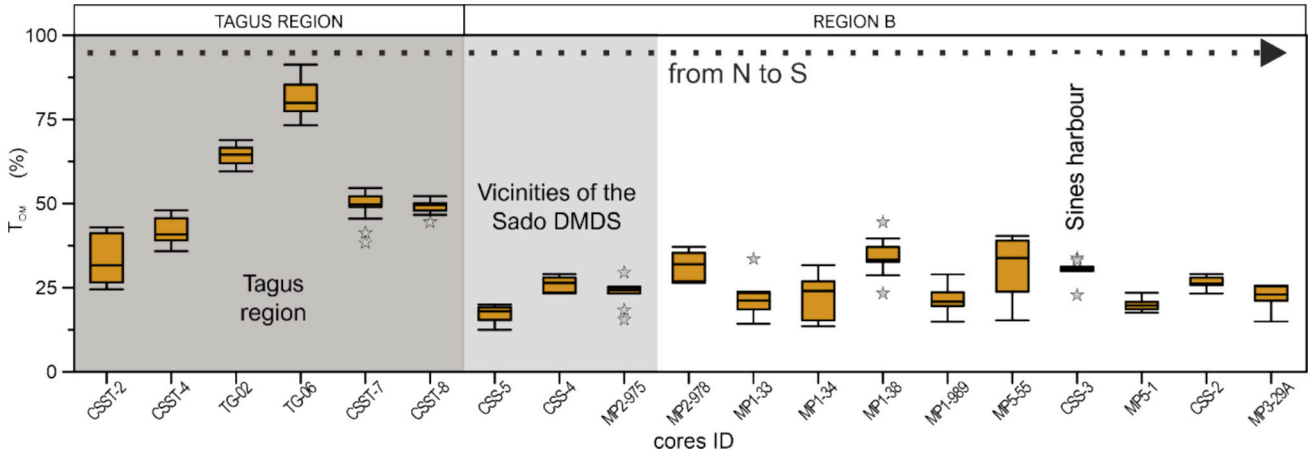

Fig. 14. Relative contribution of terrestrial OM (T_{OM}) in the sediment cores. The star symbol represent the outlier samples.

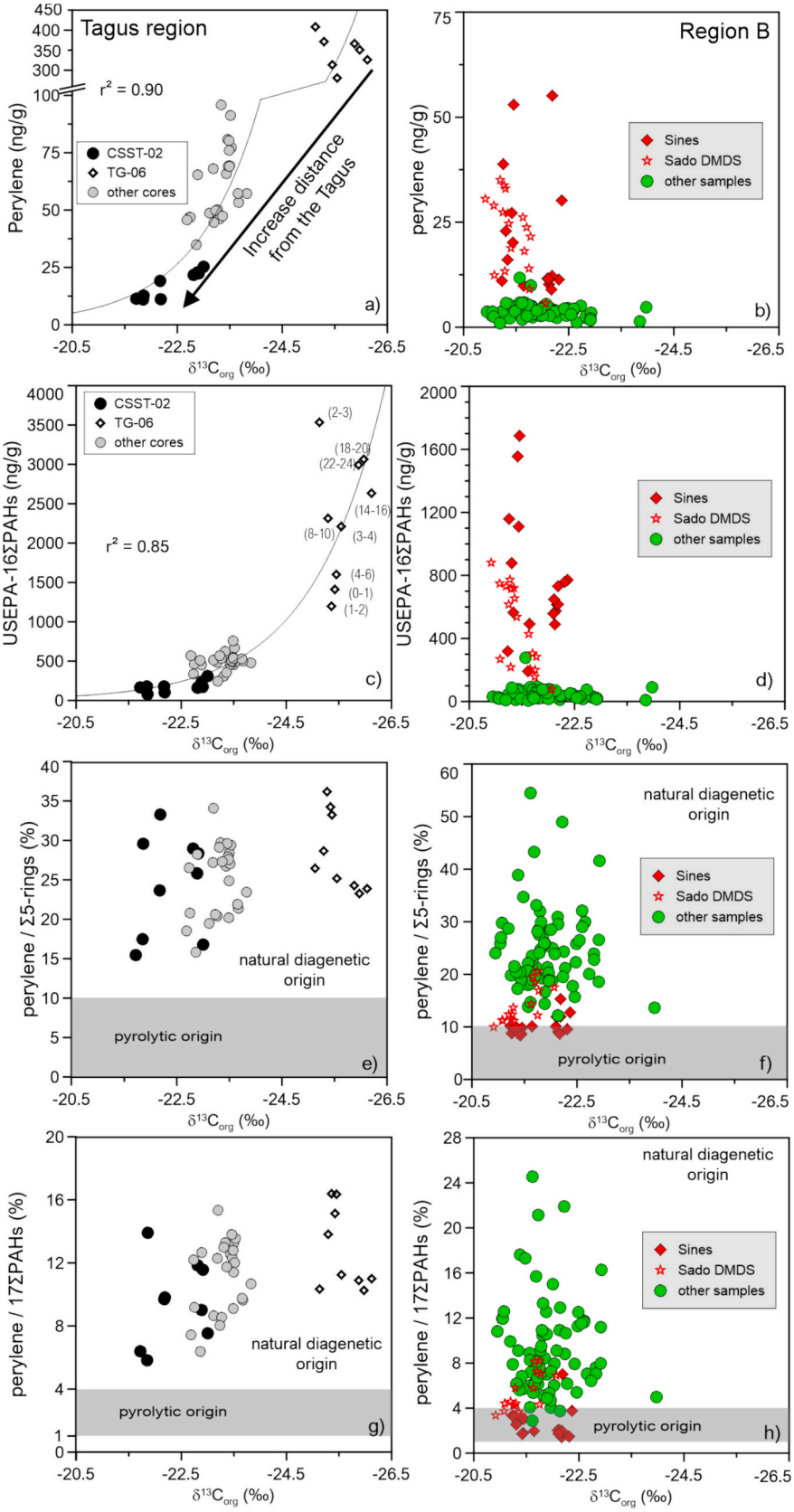

Fig. 15. $\delta^{13}C_{org}$ versus perylene, $\delta^{13}C_{org}$ versus 16ΣPAHs, $\delta^{13}C_{org}$ versus perylene/Σ5-ring PAHs and $\delta^{13}C_{org}$ versus perylene/17ΣPAHs in the sediment samples from the Tagus region (a, c, e and g) and Region B (b, d, f and h).

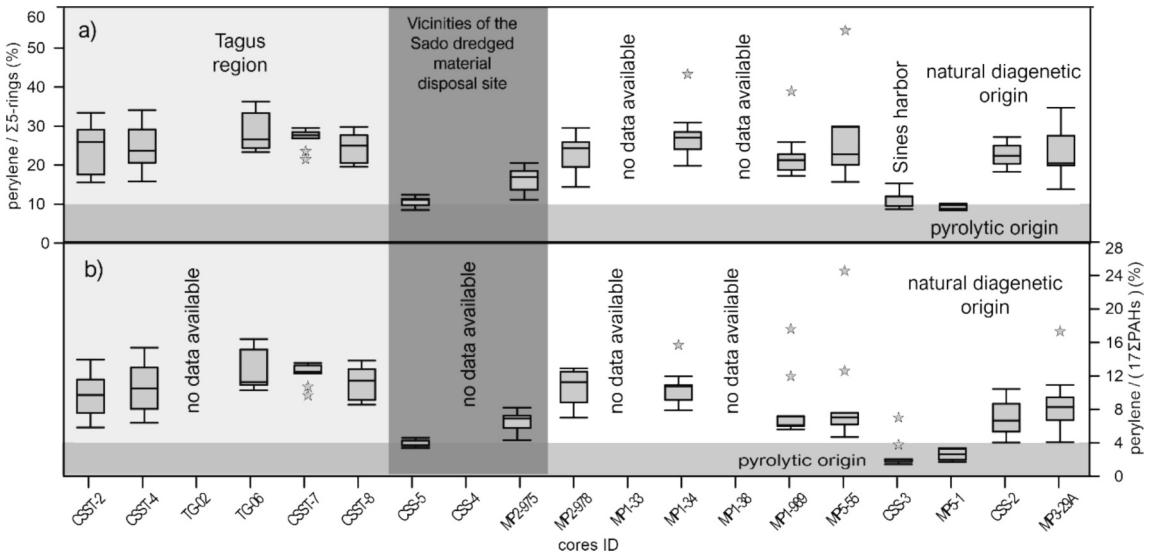

Fig. 16. Box-whisker plots for the perylene/Σ5-rings a) and perylene/(17ΣPAHs) b) in the collected sediment cores, ordered from North (left) to South (right). The star symbol represents the outlier samples. No data available means that these parameters were not measured in these cores.

et al., 2003). In the sediment samples from the Tagus region, perylene/17ΣPAHs ranged from 6 % to 16 % (median 11 %), indicating again that perylene in sediments from that region had a diagenetic origin (Fig. 15b). The USEPA-16ΣPAHs correlate positively with perylene, indicating that these compounds were subject to similar mixing and transport from the terrestrial source to the marine deposition area. Low values of perylene/17ΣPAHs occurred in three cores from Region B (Fig. 15h, Fig. 16b), two (CSS-3 and MP5-1) in the vicinity of Sines and the third (CSS-5) in the vicinity of the Sado DMDS. The median values of perylene/17ΣPAHs in these cores were 2.0 %, 2.7 %, and 3.7 %, respectively. These low values in the Sines area confined to a relatively small area, indicate that the source of perylene in these locations is most likely pyrolytic, probably derived from the oil refinery and thermoelectric power plant in Sines. In the absence of river inputs atmospheric contributions derived from the Sines industrial complex are relatively important. In core CSS-5, deposited PAH-contaminated dredged material from the Sado estuary is a probable source (Fig. 15f, Fig. 16b).

5. Conclusions

Spatial and down-core (temporal) variations were assessed in marine sediments of the Southwestern Portuguese continental shelf. The down-core variability of grain size, $CaCO_3$, C_{org}, N_{tot}, stable isotopes ($\delta^{13}C_{org}$ and $\delta^{15}N_{tot}$), perylene and USEPA-16 ΣPAHs suggested a lack of major changes occurred in the supply of terrestrial and marine sediment and OM over the past decades covered by the studied sediment cores. However, perylene and other PAHs, showed slightly increases towards the surface in some cores, suggesting variable inputs.

The spatial distributions of these proxies in surface in sediments of the Tagus region and Region B reflected variable supplies and mixing in diverse proportions of sediment particles and OM of terrestrial and marine origin. In the Tagus region, the terrestrial contribution to the OM decreased with increasing distance from the Tagus river and increasing marine OM contribution. The OM in sediments closest to the Tagus River outflow (TG-02 and TG-06) were predominated by terrestrial sources.

Perylene and the USEPA-16ΣPAHs were significantly correlated in both regions. The diagnostic ratios suggested that perylene in the Tagus region was derived from terrestrial sources, pointing to the importance of mixing processes during the transfer of the sediments from the river to the marine environment rather than a common anthropogenic source.

In the Region B, particularly nearby Sines and the Sado DMDS, the diagnostic ratios suggested that perylene had an anthropogenic pyrolytic origin. In the absence of significant river inputs in this area, perylene likely originated from atmospheric deposition derived from the Sines industrial complex. At Sado DMDS perylene likely originated from deposition of contaminated materials derived from dredged areas of the Sado estuary. The results of the present study indicated that perylene in the Tagus region may be used as is a proxy of terrestrial input to evaluate the influence of the Tagus river in the adjacent coastal area.

The multiproxy approach described in the present study provides better understanding of the origin and transport pathways of OM and contaminants in marine sediments. It supports a more accurate assessment of contaminant loads and sources, in the context of marine dynamics (e.g., MSFD), which may be of interest for application of risk assessment programs in other regions.

CRediT authorship contribution statement

Mário Mil-Homens: Writing – review & editing, Writing – original draft, Project administration, Methodology, Investigation, Funding acquisition, Formal analysis, Data curation, Conceptualization. **Sofia Gonçalves:** Writing – review & editing, Formal analysis. **Alejandro Cortes:** Formal analysis. **Barend L. van Drooge:** Writing – review & editing, Methodology, Formal analysis. **Henko de Stigter:** Writing – review & editing, Formal analysis. **Joan O. Grimalt:** Writing – review & editing, Formal analysis. **Lívia Gebara Cordeiro:** Writing – review & editing. **Miguel M. Santos:** Writing – review & editing, Formal analysis, Conceptualization. **C. Marisa R. Almeida:** Writing – review & editing, Formal analysis. **Miguel Caetano:** Writing – review & editing, Investigation, Funding acquisition.

Declaration of competing interest

The authors declare the following financial interests/personal relationships which may be considered as potential competing interests: Mario Mil Homens reports financial support was provided by Portuguese Institute for the Sea and Atmosphere. Mario Mil Homens reports a relationship with Portuguese Institute for the Sea and Atmosphere that includes: employment. If there are other authors, they declare that they have no known competing financial interests or personal relationships that could have appeared to influence the work reported in this paper.

Acknowledgments

The authors would like to thank for financial support: FEAMP through the CSS project (MAR-01.04.02-FEAMP-0013). The TAGUSGAS project (PTDC/CTA-GEO/31885/2017) and the CSS project financed the 2021 sampling campaign. The MINEPLAT project (ALT20-03-0145-FEDER-000013) supported part of the 2021 sampling campaign and the 2019 sampling campaign, respectively. Special thanks are due to the crews of the research vessel Noruega and the Portuguese Navy research vessel NRP Almirante Gago Coutinho and to all who participated in these two sampling campaigns. The authors thank the technical staff of the IPMA laboratories involved in sampling and sample preparation for the several analyses. A special thanks to Warley Soares, Mafalda Freitas and André Santana from IPMA for doing the grain-size, Corg and Ntot determinations. We also thank to Piet van Gaever from NIOZ for undertaking the ^{210}Pb and ^{226}Ra measurements. The IPMA Sedimentological Laboratory was financed by project PINFRA/22157/2016-EMSO-PT. The authors also acknowledge the Fundação para a Ciência e a Tecnologia (FCT) for CIIMAR Strategic Funding UIDB/04423/2020 and UIDP/04423/2020 and for CCMAR Strategic Funding UIDB/04326/2020, UIDP/04326/2020 and LA/P/0101/2020. We thank the three anonymous reviewers for their constructive comments that improved this manuscript.

Appendix A. Supplementary data

Supplementary data to this article can be found online at https://doi.org/10.1016/j.marpolbul.2024.117303.

Data availability

Data will be made available on request.

References

Abessa, D., Carr, R., Rachid, B., Sousa, E., Hortelani, M., Sarkis, J., 2005. Influence of a Brazilian sewage outfall on the toxicity and contamination of adjacent sediments. Mar. Pollut. Bull. 50, 875–885.

Alt-Epping, U., Mil-Homens, M., Hebbeln, D., Abrantes, F., Schneider, R.R., 2007. Provenance of organic matter and nutrient conditions on a river- and upwelling influenced shelf: a case study from the Portuguese Margin. Mar. Geol. 243, 169–179. https://doi.org/10.1016/j.margeo.2007.04.016.

Andrews, J.E., Greenaway, A.M., Dennis, P.F., 1998. Combined carbon isotope and C/N ratios as indicators of source and fate of organic matter in a poorly flushed, tropical estuary: Hunts Bay, Kingston Harbour, Jamaica. Estuar. Coast. Shelf Sci. 46, 743–756. https://doi.org/10.1006/ecss.1997.0305.

Arzola, R.G., Wynn, R.B., Lastras, G., Masson, D.G., Weaver, P.P.E., 2008. Sedimentary features and processes in the Nazare and Setubal submarine canyons west Iberian margin. Mar. Geol. 250, 64–88. https://doi.org/10.1016/j.margeo.2007.12.006.

Bajt, O., 2022. Sedimentary record of polycyclic aromatic hydrocarbons in the Gulf of Trieste (Northern Adriatic Sea) - distribution, origin and temporal trends. Front. Mar. Sci. 9. https://doi.org/10.3389/fmars.2022.946618.

Bakhtiari, A.R., Zakaria, M.P., Yaziz, M.I., Lajis, M.N.H., Bi, X., Rahim, M.C.A., 2009. Vertical distribution and source identification of polycyclic aromatic hydrocarbons in anoxic sediment cores of Chini Lake, Malaysia: Perylene as indicator of land plant-derived hydrocarbons. Appl. Geochem. 24, 1777–1787. https://doi.org/10.1016/j.apgeochem.2009.05.008.

Barros, G.V., Martinelli, L.A., Oliveira Novais, T.M., Ometto, J.P.H.B., Zuppi, G.M., 2010. Stable isotopes of bulk organic matter to trace carbon and nitrogen dynamics in an estuarine ecosystem in Babitonga Bay (Santa Catarina, Brazil). Sci. Total Environ. 408, 2226–2232. https://doi.org/10.1016/j.scitotenv.2010.01.060.

Benito, G., Sopenã, A., Sánchez-Moya, Y., Machado, M., Pérez-González, 2003. Palaeoflood record of the Tagus River (Central Spain) during the Late Pleistocene and Holocene. Quat. Sci. Rev. 22, 1737–1756. https://doi.org/10.1016/S0277-3791(03)00133-1.

Bianchi, T.S., Mitra, S., McKee, B.A., 2002. Sources of terrestrially-derived organic carbon in lower Mississippi River and Louisiana shelf sediments: implications for differential sedimentation and transport at the coastal margin. Mar. Chem. 77, 211–223. https://doi.org/10.1016/S0304-4203(01)00088-3.

Birch, G.F., 2020. An assessment of aluminum and iron in normalisation and enrichment procedures for environmental assessment of marine sediment. Sci. Total Environ. 727, 138123. https://doi.org/10.1016/j.scitotenv.2020.138123.

Boer, W., Van Den Bergh, G.D., De Haas, H., De Stigter, H.C., Gieles, R., Van Weering, T. C.E., 2006. Validation of accumulation rates in Teluk Banten (Indonesia) from commonly applied ^{210}Pb models, using the 1883 Krakatau tephra as time marker. Mar. Geol. 227, 263–277. https://doi.org/10.1016/j.margeo.2005.12.002.

Burdige, D.J., 2007. Preservation of organic matter in marine sediments: controls, mechanisms, and an imbalance in sediment organic carbon budgets? Chem. Rev. 107, 467–485. https://doi.org/10.1021/cr050347q.

Caeiro, S., Costa, M.H., Ramos, T.B., Fernandes, F., Silveira, N., Coimbra, A., Medeiros, G., Painho, M., 2005. Assessing heavy metal contamination in Sado estuary sediment: an index analysis approach. Ecol. Indic. 5, 151–169. https://doi.org/10.1016/j.ecolind.2005.02.001.

Caetano, M., Raimundo, J., Nogueira, M., Santos, M., Mil-Homens, M., Prego, R., Vale, C., 2016. Defining benchmark values for nutrients under the water framework directive: application in twelve Portuguese estuaries. Mar. Chem. 185, 27–37. https://doi.org/10.1016/j.marchem.2016.05.002.

Canário, J., Vale, C., Caetano, M., 2005. Distribution of monomethylmercury and mercury in surface sediments of the Tagus estuary (Portugal). Mar. Pollut. Bull. 50, 1142–1145. https://doi.org/10.1016/j.marpolbul.2005.06.052.

Carpenter, R., Peterson, M.L., Bennett, J.T., 1982. ^{210}Pb-derived sediment accumulation and mixing rates for the Washington continental slope. Mar. Geol. 48, 135–164. https://doi.org/10.1016/0025-3227(82)90133-5.

Chen, S.J., Luo, X.J., Mai, B.X., Sheng, G.Y., Fu, J.M., Zeng, E.Y., 2006. Distribution and mass inventories of polycyclic aromatic hydrocarbons and organochlorine pesticides in sediments of the pearl river estuary and the northern South China Sea. Environ. Sci. Technol. 40, 709–714. https://doi.org/10.1021/es052060g.

Chen, C.F., Chen, C.W., Albarico, F.P.J.B., Lee, S.H., Hsu, C.W., Dong, C. Di, 2024. Sediment organic matter predicts polycyclic aromatic hydrocarbon distribution in port sediments. Mar. Pollut. Bull. 207, 116869. https://doi.org/10.1016/J.MARPOLBUL.2024.116869.

Cobelo-García, A., Neira, P., Mil-Homens, M., Caetano, M., 2011. Evaluation of the contamination of platinum in estuarine and coastal sediments (Tagus Estuary and Prodelta, Portugal). Mar. Pollut. Bull. 62, 646–650. https://doi.org/10.1016/j.marpolbul.2010.12.018.

Costa, A.M., Mil-Homens, M., Lebreiro, S.M., Richter, T.O., de Stigter, H., Boer, W., Trancoso, M.A., Melo, Z., Mouro, F., Mateus, M., Canário, J., Branco, V., Caetano, M., 2011. Origin and transport of trace metals deposited in the canyons off Lisboa and adjacent slopes (Portuguese Margin) in the last century. Mar. Geol. 282, 169–177. https://doi.org/10.1016/j.margeo.2011.02.007.

de Stigter, H.C., Boer, W., de Jesus Mendes, P.A., Jesus, C.C., Thomsen, L., van den Bergh, G.D., van Weering, T.C.E., 2007. Recent sediment transport and deposition in the Nazaré Canyon, Portuguese continental margin. Mar. Geol. 246, 144–164. https://doi.org/10.1016/j.margeo.2007.04.011.

Fang, M. Der, Lee, C.L., Yu, C.S., 2003. Distribution and source recognition of polycyclic aromatic hydrocarbons in the sediments of Hsin-ta Harbour and adjacent coastal areas, Taiwan. Mar. Pollut. Bull. 46, 941–953. https://doi.org/10.1016/S0025-326X(03)00099-7.

Ferreira, J.G., Simas, T., Nobre, A., Silva, M.C., Sifferegger, K., Lencart-Silva, J., 2003. Identificarion of Sensitive and Vulnerable Zones in Transitional and Coastal Portuguese Systems. INAG and IMAR.

Figueres, G., Martin, J.M., Meybeck, M., Seyler, P., 1985. A comparative study of mercury contamination in the Tagus estuary (Portugal) and major French estuaries (Gironde, Loire, Rhône). Estuar. Coast. Shelf Sci. 20, 183–203. https://doi.org/10.1016/0272-7714(85)90037-X.

Fiúza, A., 1983. Upwelling patterns of Portugal. In: Suess, E., Thiede, J. (Eds.), Coastal Upwelling, Its Sedimentary Record. Part A. Responses of the Sedimentary Regime to Present Coast. Plenum Press, New York, pp. 85–98.

Fiúza, A., Macedo, M., Guerreiro, M., 1982. Climatological space and time variation of the Portuguese coastal upwelling. Oceanol. Acta 5, 31–40.

Gao, X., Yang, Y., Wang, C., 2012. Geochemistry of organic carbon and nitrogen in surface sediments of coastal Bohai Bay inferred from their ratios and stable isotopic signatures. Mar. Pollut. Bull. 64, 1148–1155. https://doi.org/10.1016/j.marpolbul.2012.03.028.

Gaspar, L.C., Monteiro, J.H., 1977. Materia orgânica nos sedimentos da plataforma continental portuguesa entre os cbos Espichel e Raso. Comun. dos Serviços Geológicos Port. 62, 69–83.

Gocht, T., Barth, J.A.C., Epp, M., Jochmann, M., Blessing, M., Schmidt, T.C., Grathwohl, P., 2007. Indications for pedogenic formation of perylene in a terrestrial soil profile: depth distribution and first results from stable carbon isotope ratios. Appl. Geochem. 22, 2652–2663. https://doi.org/10.1016/j.apgeochem.2007.06.004.

Gonçalves, C., Teixeira, C., Basto, M.C.P., Almeida, C.M.R., 2016. PAHs levels in Portuguese estuaries and lagoons: salt marsh plants as potential agents for the containment of PAHs contamination in sediments. Reg. Stud. Mar. Sci. 7, 211–221. https://doi.org/10.1016/j.rsma.2016.05.004.

Goñi, M.A., Ruttenberg, K.C., Eglinton, T.I., 1998. A reassessment of the sources and importance of land-derived organic matter in surface sediments from the Gulf of Mexico. Geochim. Cosmochim. Acta 62, 3055–3075. https://doi.org/10.1016/S0016-7037(98)00217-8.

Haffert, L., Haeckel, M., De Stigter, H., Janssen, F., 2020. Assessing the temporal scale of deep-sea mining impacts on sediment biogeochemistry. Biogeosciences 17, 2767–2789. https://doi.org/10.5194/bg-17-2767-2020.

Hanke, U.M., Lima-Braun, A.L., Eglinton, T.I., Donnelly, J.P., Galy, V., Poussart, P., Hughen, K., McNichol, A.P., Xu, L., Reddy, C.M., 2019. Significance of perylene for source allocation of terrigenous organic matter in aquatic sediments. Environ. Sci. Technol. 53, 8244–8251. https://doi.org/10.1021/acs.est.9b02344.

Hedges, J.I., Clark, W.A., Come, G.L., 1988. Organic matter sources to the water column and surficial sediments of a marine bay. Limnol. Oceanogr. 33, 1116–1136. https://doi.org/10.4319/lo.1988.33.5.1116.

Heyes, A., Mason, R.P., Kim, E.-H., Sunderland, E., 2006. Mercury methylation in estuaries: insights from using measuring rates using stable mercury isotopes. Mar. Chem. 102, 134–147.

Hu, L., Shi, X., Lin, T., Guo, Z., Ma, D., Yang, Z., 2014. Perylene in surface sediments from the estuarine-inner shelf of the East China Sea: a potential indicator to assess the sediment footprint of large river influence. Cont. Shelf Res. 90, 142–150. https://doi.org/10.1016/j.csr.2014.04.014.

Jouanneau, J.M., Garcia, C., Oliveira, A., Rodrigues, A., Dias, J.A., Weber, O., 1998. Dispersal and deposition of suspended sediment on the shelf off the Tagus and Sado estuaries, S.W. Portugal. Prog. Oceanogr. 42, 233–257. https://doi.org/10.1016/S0079-6611(98)00036-6.

Lamb, A.L., Wilson, G.P., Leng, M.J., 2006. A review of coastal palaeoclimate and relative sea-level reconstructions using δ13C and C/N ratios in organic material. Earth-Science Rev. 75, 29–57. https://doi.org/10.1016/j.earscirev.2005.10.003.

Li, Z., Huang, H., Yan, G., Xu, Y., George, S.C., 2022. Occurrence and origin of perylene in Paleogene sediments from the Tasmanian Gateway, Australia. Org. Geochem. 168, 104406. https://doi.org/10.1016/j.orggeochem.2022.104406.

Lima, L., 1971. Distribuição dos minerais argilosos na plataforma continental entre os cabos Raso e Espichel. In: 1º Congresso Hispano-Luso-Americano de Geologia Económica. Madrid.

Lima, A.L.C., Eglinton, T.I., Reddy, C.M., 2003. High-resolution record of pyrogenic polycyclic aromatic hydrocarbon deposition during the 20th century. Environ. Sci. Technol. 37, 53–61. https://doi.org/10.1021/es025895p.

Liu, L.-Y., Wang, J.-Z., Wei, G.-L., Guan, Y.-F., Wong, C.S., Zeng, E.Y., 2012. Sediment records of polycyclic aromatic hydrocarbons (PAHs) in the continental shelf of China: implications for evolving anthropogenic impacts. Environ. Sci. Technol. 46, 6497–6504. https://doi.org/10.1021/es300474z.

Liu, D., Li, X., Emeis, K.C., Wang, Y., Richard, P., 2015. Distribution and sources of organic matter in surface sediments of Bohai Sea near the Yellow River Estuary, China. Estuar. Coast. Shelf Sci. 165, 128–136. https://doi.org/10.1016/j.ecss.2015.09.007.

Logemann, A.E., Röhrs, S., Brockmeyer, B., 2023. Distribution of hydrophobic organic contaminants in marine sediment fines—an alternative normalization strategy? Integr. Environ. Assess. Manag. 19, 1348–1360. https://doi.org/10.1002/ieam.4744.

Luo, X.J., Chen, S.J., Mai, B.X., Yang, Q.S., Sheng, G.Y., Fu, J.M., 2006. Polycyclic aromatic hydrocarbons in suspended particulate matter and sediments from the Pearl River Estuary and adjacent coastal areas, China. Environ. Pollut. 139, 9–20. https://doi.org/10.1016/j.envpol.2005.05.001.

MAOTDR, 2007. Ordinance 1450/2007. "Portaria 1450/2007, de 12 de novembro". Emission by Ministério do Ambiente, do Ordenamento do Território e do Desenvolvimento Regiona, pp. 8372–8382. Diário da República 217/2007, Série I. https://dre.pt/dre/detalhe/portaria/1450-2007-629400.

Mayer, L.M., 1994. Surface area control of organic carbon accumulation in continental shelf sediments. Geochim. Cosmochim. Acta 58, 1271–1284. https://doi.org/10.1016/0016-7037(94)90381-6.

Meyers, P.A., 1994. Preservation of elemental and isotopic source identification of sedimentary organic matter. Chem. Geol. 114, 289–302. https://doi.org/10.1016/0009-2541(94)90059-0.

Meyers, P.A., 1997. Organic geochemical proxies of paleoceanographic, paleolimnologic, and paleoclimatic processes. In: Organic Geochemistry. Pergamon, pp. 213–250. https://doi.org/10.1016/S0146-6380(97)00049-1.

Mil-Homens, M., Stevens, R.L., Boer, W., Abrantes, F., Cato, I., 2006. Pollution history of heavy metals on the Portuguese shelf using ^{210}Pb-geochronology. Sci. Total Environ. 367, 466–480. https://doi.org/10.1016/j.scitotenv.2006.03.042.

Mil-Homens, M., Branco, V., Vale, C., Boer, W., Alt-Epping, U., Abrantes, F., Vicente, M., 2009. Sedimentary record of anthropogenic metal inputs in the Tagus prodelta (Portugal). Cont. Shelf Res. 29, 381–392. https://doi.org/10.1016/j.csr.2008.10.002.

Mil-Homens, M., Blum, J., Canário, J., Caetano, M., Costa, A.M., Lebreiro, S.M., Trancoso, M., Richter, T., de Stigter, H., Johnson, M., Branco, V., Cesário, R., Mouro, F., Mateus, M., Boer, W., Melo, Z., 2013. Tracing anthropogenic Hg and Pb input using stable Hg and Pb isotope ratios in sediments of the central Portuguese Margin. Chem. Geol. 336, 62–71. https://doi.org/10.1016/j.chemgeo.2012.02.018.

Moita, M.T., Oliveira, P.B., Mendes, J.C., Palma, A.S., 2003. Distribution of chlorophyll a and Gymnodinium catenatum associated with coastal upwelling plumes off central Portugal. In: Acta Oecologica. Elsevier, Masson, pp. S125–S132. https://doi.org/10.1016/S1146-609X(03)00011-0.

Moreno-González, R., Rodriguez-Mozaz, S., Gros, M., Barceló, D., León, V.M., 2015. Seasonal distribution of pharmaceuticals in marine water and sediment from a mediterranean coastal lagoon (SE Spain). Environ. Res. 138, 326–344. https://doi.org/10.1016/j.envres.2015.02.016.

Owens, N.J.P., 1988. Natural variations in 15N in the marine environment. Adv. Mar. Biol. 24, 389–451. https://doi.org/10.1016/S0065-2881(08)60077-2.

Pang, S.Y., Suratman, S., Latif, M.T., Khan, M.F., Simoneit, B.R.T., Mohd Tahir, N., 2022. Polycyclic aromatic hydrocarbons in coastal sediments of Southern Terengganu, South China Sea, Malaysia: source assessment using diagnostic ratios and multivariate statistic. Environ. Sci. Pollut. Res. 29, 15849–15862. https://doi.org/10.1007/s11356-021-16762-6.

Perdue, E.M., Koprivnjak, J.F., 2007. Using the C/N ratio to estimate terrigenous inputs of organic matter to aquatic environments. Estuar. Coast. Shelf Sci. 73, 65–72. https://doi.org/10.1016/j.ecss.2006.12.021.

Quaresma, L., Vitorino, J., da Silva, J., Union, E.G., 2005. Non-linear internal waves generated at Nazaré canyon: observations over the W Portuguese inner shelf. In: Union, E.G. (Ed.), European Geosciences Union, General Assembly 2005, p. 10135. Vienna, Austria.

Quaresma, L.S., Vitorino, J., Oliveira, A., da Silva, J., 2007. Evidence of sediment resuspension by nonlinear internal waves on the western Portuguese mid-shelf. Mar. Geol. 246, 123–143. https://doi.org/10.1016/J.MARGEO.2007.04.019.

Readman, J.W., Fillmann, G., Tolosa, I., Bartocci, J., Villeneuve, J.P., Catinni, C., Mee, L.D., 2002. Petroleum and PAH contamination of the Black Sea. Mar. Pollut. Bull. 44, 48–62. https://doi.org/10.1016/S0025-326X(01)00189-8.

Rocha, A.C., Palma, C., 2019. Source identification of polycyclic aromatic hydrocarbons in soil sediments: application of different methods. Sci. Total Environ. 652, 1077–1089. https://doi.org/10.1016/j.scitotenv.2018.10.014.

Rocha, M.J., Dores-Sousa, J.L., Cruzeiro, C., Rocha, E., 2017. PAHs in water and surface sediments from Douro River estuary and Porto Atlantic coast (Portugal)—impacts on human health. Environ. Monit. Assess. 189, 1–14. https://doi.org/10.1007/s10661-017-6137-6.

Rumolo, P., Barra, M., Gherardi, S., Marsella, E., Sprovieri, M., 2011. Stable isotopes and C/N ratios in marine sediments as a tool for discriminating anthropogenic impact. J. Environ. Monit. 13, 3399–3408. https://doi.org/10.1039/c1em10568j.

Sampaio, L., Freitas, R., Máguas, C., Rodrigues, A., Quintino, V., 2010. Coastal sediments under the influence of multiple organic enrichment sources: an evaluation using carbon and nitrogen stable isotopes. Mar. Pollut. Bull. 60, 272–282. https://doi.org/10.1016/j.marpolbul.2009.09.008.

Sampaio, L., Mamede, R., Ricardo, F., Magalhães, L., Rocha, H., Martins, R., Dauvin, J.C., Rodrigues, A.M., Quintino, V., 2016. Soft-sediment crustacean diversity and distribution along the Portuguese continental shelf. J. Mar. Syst. 163, 43–60. https://doi.org/10.1016/j.jmarsys.2016.06.011.

Schmidt, F., Hinrichs, K.U., Elvert, M., 2010. Sources, transport, and partitioning of organic matter at a highly dynamic continental margin. Mar. Chem. 118, 37–55. https://doi.org/10.1016/j.marchem.2009.10.003.

Schubert, C.J., Calvert, S.E., 2001. Nitrogen and carbon isotopic composition of marine and terrestrial organic matter in Arctic Ocean sediments: implications for nutrient utilization and organic matter composition. Deep Res. Part I Oceanogr. Res. Pap. 48, 789–810. https://doi.org/10.1016/S0967-0637(00)00069-8.

Shultz, D.J., Calder, J.A., 1976. Organic carbon 13C12C variations in estuarine sediments. Geochim. Cosmochim. Acta 40, 381–385. https://doi.org/10.1016/0016-7037(76)90002-8.

Silliman, J.E., Meyers, P.A., Ostrom, P.H., Ostrom, N.E., Eadie, B.J., 2000. Insights into the origin of perylene from isotopic analyses of sediments from Saanich Inlet, British Columbia. Org. Geochem. 31, 1133–1142. https://doi.org/10.1016/S0146-6380(00)00120-0.

Simpson, C.D., Mosi, A.A., Cullen, W.R., Reimer, K.J., 1996. Composition and distribution of polycyclic aromatic hydrocarbon contamination in surficial marine sediments from Kitimat Harbor, Canada. Sci. Total Environ. 181, 265–278. https://doi.org/10.1016/0048-9697(95)05026-4.

Stein, R., 1991. Accumulation of organic carbon in marine sediments: results from the Deep Sea Drilling Project/Ocean Drilling Program (DSDP/ODP). Springer-Verlag, Heidelberg. https://doi.org/10.1007/BFb0010382.

Stein, R., Rack, F.R., 1995. A 160,000-year high-resolution record of quantity and composition of organic carbon in the Santa Barbara Basin (site 893). In: Kennett, J., Baldauf, J., Lyle, M. (Eds.), Proceedings of the Ocean Drilling Program, 146 Part 2 Scientific Results, pp. 125–138. https://doi.org/10.2973/odp.proc.sr.146-2.298.1995.

Sun, X., Hu, L., Fan, D., Wang, H., Yang, Z., Guo, Z., 2024. Sediment resuspension accelerates the recycling of terrestrial organic carbon at a large river-coastal ocean interface. Glob. Biogeochem. Cycles 38. https://doi.org/10.1029/2024GB008213.

Vale, C., Cortesão, C., Castro, O., Ferreira, A.M., 1993. Suspended-sediment response to pulses in river flow and semidiurnal and fortnightly tidal variations in a mesotidal estuary. Mar. Chem. 43, 21–31. https://doi.org/10.1016/0304-4203(93)90213-8.

Van Drooge, B.L., López, J., Fernández, P., Grimalt, J.O., Stuchlík, E., 2011. Polycyclic aromatic hydrocarbons in lake sediments from the High Tatras. Environ. Pollut. 159, 1234–1240. https://doi.org/10.1016/j.envpol.2011.01.035.

Vanney, J.-R., Mougenot, D., 1981. La plate-forme continentale du Portugal et les provinces adjacentes: Analyse Geomorphologique. Memórias dos Serviços Geológicos Port. 28, 86 pp.

Varnosfaderany, M.N., Bakhtiari, A.R., Gu, Z., Chu, G., 2014. Perylene as an indicator of land-based plant biomarkers in the southwest Caspian Sea. Mar. Pollut. Bull. 80, 124–131. https://doi.org/10.1016/j.marpolbul.2014.01.033.

Venkatesan, M.I., 1988. Occurrence and possible sources of perylene in marine sediments-a review. Mar. Chem. 25, 1–27. https://doi.org/10.1016/0304-4203(88)90011-4.

Venkatesan, M.I., Chalaux, N., Bayona, J.M., Zeng, E., 1998. Butyltins in sediments from Santa Monica and San Pedro basins, California. Environ. Pollut. 99, 263–269. https://doi.org/10.1016/S0269-7491(97)00136-X.

Viñas, L., Angeles Franco, M., Antonio Soriano, J., José González, J., Pon, J., Albaigés, J., 2010. Sources and distribution of polycyclic aromatic hydrocarbons in sediments from the Spanish northern continental shelf. Assessment of spatial and temporal trends. Environ. Pollut. 158, 1551–1560. https://doi.org/10.1016/j.envpol.2009.12.023.

Wakeham, S.G., Schaffner, C., Giger, W., Boon, J.J., De Leeuw, J.W., 1979. Perylene in sediments from the Namibian shelf. Geochim. Cosmochim. Acta 43, 1141–1144. https://doi.org/10.1016/0016-7037(79)90100-5.

Wang, C., Lv, Y., Li, Y., 2018. Riverine input of organic carbon and nitrogen in water-sediment system from the Yellow River estuary reach to the coastal zone of Bohai Sea, China. Cont. Shelf Res. 157, 1–9. https://doi.org/10.1016/j.csr.2018.02.004.

Winkelmann, D., Knies, J., 2005. Recent distribution and accumulation of organic carbon on the continental margin west off Spitsbergen. Geochem. Geophys. Geosyst. 6. https://doi.org/10.1029/2005GC000916.

Xia, J., Han, Y., Tan, J., Abarike, G.A., Song, Z., 2022. The characteristics of organic carbon in the offshore sediments surrounding the Leizhou Peninsula, China. Front. Earth Sci. 10. https://doi.org/10.3389/feart.2022.648337.

Zakrzewski, A., Kosakowski, P., Waliczek, M., Kowalski, A., 2020. Polycyclic aromatic hydrocarbons in Middle Jurassic sediments of the Polish Basin provide evidence for high-temperature palaeo-wildfires. Org. Geochem. 145. https://doi.org/10.1016/j.orggeochem.2020.104037.

Zhang, X., Xu, Y., Ruan, J., Ding, S., Huang, X., 2014. Origin, distribution and environmental significance of perylene in Okinawa Trough since last glaciation maximum. Org. Geochem. 76, 288–294. https://doi.org/10.1016/j.orggeochem.2014.09.008.

Zhang, R., Li, T., Russell, J., Zhang, F., Xiao, X., Cheng, Y., Liu, Z., Guan, M., Han, Q., 2020. Source apportionment of polycyclic aromatic hydrocarbons in continental shelf of the East China Sea with dual compound-specific isotopes (δ13C and δ2H). Sci. Total Environ. 704, 135459. https://doi.org/10.1016/j.scitotenv.2019.135459.

Zhao, C., Jiang, Z., Wu, Y., Liu, S., Cui, L., Zhang, J., Huang, X., 2019. Origins of sediment organic matter and their contributions at three contrasting wetlands in a coastal semi-enclosed ecosystem. Mar. Pollut. Bull. 139, 32–39. https://doi.org/10.1016/J.MARPOLBUL.2018.12.008.

Ziebis, W., Forster, S., Huettel, M., Jørgensen, B.B., 1996. Complex burrows of the mud shrimp Callianassa truncata and their geochemical impact in the sea bed. Nature 382, 619–622. https://doi.org/10.1038/382619a0.